

AQUACULTURE AND THE BENTHIC HABITAT: BAY-SCALE VARIABILITY IN  
RESPONSE TO ORGANIC LOADING AND NOVEL APPROACHES TO INFORM  
REGULATORY MONITORING PRACTICES

By

J.F. Hart Koepke

Submitted in partial fulfillment of the requirements  
for the degree of Master of Science

at

Dalhousie University  
Halifax, Nova Scotia  
August 2021

© Copyright by J.F. Hart Koepke, 2021

*Dedicated to my family*

# TABLE OF CONTENTS

<b>List of Tables</b> .....	vi
<b>List of Figures</b> .....	vii
<b>Abstract</b> .....	viii
<b>List of Abbreviations and Symbols Used</b> .....	ix
<b>Acknowledgements</b> .....	x
<b>Chapter 1. Introduction</b> .....	1
1.1 Outline and Objectives.....	5
<b>Chapter 2. Comparative Analysis of Finfish Aquaculture Sites Within Shelburne Bay, Nova Scotia</b> .....	7
2.1 Introduction.....	7
2.2 Methods.....	10
2.2.1 Study Sites.....	10
2.2.2 Field Methods.....	12
2.2.3 Acoustics.....	13
2.2.4 Laboratory Methods.....	14
2.2.5 Statistical Analysis.....	16
2.3 Results.....	17
2.3.1 Sediment Geochemistry.....	17
2.3.1.1 Grain Size.....	17
2.3.1.2 Spatiotemporal Patterns: Present Study.....	18
2.3.1.3 Spatiotemporal Patterns: Historical Monitoring Data.....	25
2.3.2 Geochemical Correlations.....	33

2.3.3 Acoustic Bottom Signatures.....	36
2.4 Discussion.....	38
2.4.1 Spatial and Temporal Variability.....	38
2.4.2 EMP Vs. Present Study.....	42
2.4.3 Geochemical Relationships.....	43
2.4.4 Acoustics.....	44
2.4.5 Ecosystem Approach to Aquaculture.....	45
<b>Chapter 3. DIAGENIX: Benthic Diagenesis Modelling to Inform Environmental Management Strategies.....</b>	<b>47</b>
3.1 Introduction.....	47
3.2 Methods.....	51
3.2.1 DIAGENIX Structure.....	51
3.2.2 Parameterization.....	56
3.2.3 Initial Conditions.....	58
3.2.4 Validation.....	58
3.2.5 Simulations.....	60
3.2.6 Sensitivity.....	61
3.3 Results.....	61
3.3.1 Initial State.....	61
3.3.2 Organic Matter Pool Ratio.....	62
3.3.3 Mineralisation Rates.....	64
3.3.4 Transport Parameters.....	66
3.3.5 Validation.....	68
3.3.6 Sensitivity.....	70

3.4 Discussion.....	70
3.4.1 Farm Deposition & Mineralisation.....	71
3.4.2 Validation.....	73
3.4.3 Biological Transport.....	76
3.4.4 Recovery.....	78
3.4.5 Future Applications.....	79
<b>Chapter 4. Conclusions.....</b>	<b>81</b>
<b>Works Cited.....</b>	<b>84</b>
<b>Appendix.....</b>	<b>93</b>
A.1 Clustering Validation Methods.....	93
A.2 O <sub>2</sub> vs. SO <sub>4</sub> Pathway Quantification.....	95

## LIST OF TABLES

<b>Table 2.1:</b> List of relevant farm aspects for each study site.....	12
<b>Table 2.2:</b> Grain size results.....	18
<b>Table 2.3:</b> Kruskal-Wallis comparison results between present study and EMP data.....	27
<b>Table 2.4:</b> Kruskal-Wallis comparison results between lease and reference sites for EMP data.....	29
<b>Table 2.5:</b> Empirical relationship summary of dissolved sulfides and redox potential.....	34
<b>Table 3.1:</b> Idealized set of primary and secondary redox reactions in DIAGENIX.....	52
<b>Table 3.2:</b> Summary of model equations.....	54
<b>Table 3.3:</b> Summary of rate equations.....	54
<b>Table 3.4:</b> Model parameters and boundary conditions used in DIAGENIX.....	57
<b>Table A.1:</b> Percent total of sulfate reduction and oxic respiration.....	95

## LIST OF FIGURES

<b>Figure 2.1:</b> Map of study sites.....	11
<b>Figure 2.2:</b> Maps of sample locations for each lease.....	13
<b>Figure 2.3:</b> Echo-sounding transects for each lease.....	14
<b>Figure 2.4:</b> Present study geochemical results for McNutts lease.....	20
<b>Figure 2.5:</b> Present study geochemical results for Hartz lease.....	22
<b>Figure 2.6:</b> Present study geochemical results for Sandy lease.....	24
<b>Figure 2.7:</b> Historical EMP geochemical results for all three leases.....	26
<b>Figure 2.8:</b> Empirical relationships between dissolved sulfides and redox potential.....	35
<b>Figure 2.9:</b> Bottom signature results for all three leases.....	37
<b>Figure 3.1:</b> Reaction network of chemical species interaction in DIAGENIX.....	53
<b>Figure 3.2:</b> Initial state vertical profiles of chemical species in DIAGENIX.....	62
<b>Figure 3.3:</b> Dissolved sulfides and POM content for variable organic matter pool ratio simulations.....	63
<b>Figure 3.4:</b> Dissolved sulfides and POM content for variable labile mineralisation rate simulations.....	65
<b>Figure 3.5:</b> Dissolved sulfides and POM content for variable transport parameter simulations.....	67
<b>Figure 3.6:</b> Dissolved sulfides and POM content for simulation to field observation comparison for validation.....	69

## **ABSTRACT**

Frequent assessment and revision of environmental regulatory methods is necessary to promote a sustainable approach to ecosystem management. This thesis focused on benthic monitoring practices presently utilized by the Nova Scotian government for regulating aquaculture sites and proposes enhanced and novel approaches for consideration during method revisions. The first study analyzed geochemical response of the sediment to organic loading from intermittent aquaculture activity at three sites within Shelburne Bay. Results showed notable distinctions between the sites when analyzed at both annual and multiweek timescales, as well as differences between the dissolved sulfide and redox potential relationships presented in regulatory documentation. The second study expanded on the first by utilizing monitoring data from the sites to development a benthic diagenesis model, focusing on the accumulation of dissolved sulfides in response to organic loading. Model results fit well with provincial monitoring data, but future use will require parameter tunings for individual sites.



## LIST OF ABBREVIATIONS AND SYMBOLS USED

---

<u>Abbreviation</u>	<u>Description</u>
aw	Ashed Weight
AAR	Aquaculture Activities Regulations
BW	Bottom Water
C <sub>org</sub>	Organic Carbon
DO	Dissolved Oxygen
dw	Dry Weight
EAA	Ecosystem Approach to Aquaculture
EMP	Environmental Monitoring Program
HSC	Half-Saturation Constant
ISE	Ion-Selective Electrode
NSDFA	Nova Scotia Department of Fisheries and Aquaculture
OM	Organic Matter
ORP	Oxidation-Reduction Potential
PDE	Partial Differential Equation
POM	Particulate Organic Matter
RSE	Residual Standard Error
SAOB	Sulfide Antioxidant Buffer
SWI	Sediment Water Interface
ww	Wet Weight

## ACKNOWLEDGEMENTS

First, I would like to thank my supervisor, Jon Grant, and the rest of my advisory committee, Ramón Filgueira, and Chris Algar. My committee provided me with the direction and scope necessary to bring this thesis to fruition. This thesis took on many forms throughout its life, but we were finally able to nail it down into something coherent and informative.

I would like to thank Anne McKee, Stephen Finnis, Connor Mackie, and Leigh Howarth for taking the time to assist me in gathering my field samples. Additionally, I would like to thank everyone in our lab: Donghui Jiang, Jenny Weitzman, Meredith Burke, Marianne Parent, Caitlin Stockwell, Megan Rector, Jennie Korus, Chantal Giroux, and David Greenberg for all the help they provided along the way.

And many thanks to everyone in the Department of Oceanography for ensuring my success, in ways too numerous to count. My fieldwork would not have been possible without the collaborative efforts of everyone at Cooke Aquaculture, and for that I am grateful.

# **CHAPTER 1**

## **INTRODUCTION**

Finfish aquaculture sites are becoming more prevalent worldwide in response to the rise in stress to wild fishery stocks and food requirements of a growing population (Pinsky et al., 2011). These increasing stressors will continue to drive the expansion and evolution of aquaculture if given the opportunity. Therefore, any responsible planning and management strategies must address current shortcomings before upscaling renders certain approaches unfeasible. Aquacultural practices have been under scrutiny of the general public since they began to be considered as a serious alternative to wild fisheries, with environmental awareness and a mindset of sustainability being two areas of major concern for communities where aquaculture sites are active and for seafood consumers in general (Froehlich et al., 2017). In the context of the present research, sustainability will refer to maintaining the interwoven biological, chemical, and physical systems of an environment that keep it in balance. If the presence of industry within the environment is too great, it can cause alterations in one or more of these systems and result in a domino effect across all systems that may not be easily reversed. Evaluating the influence of fish farms on the environment is instrumental in development of environmental management strategies that can be used to work towards sustainable outcomes by helping determine location, stocking density, and fallowing periods between harvests (Chamberlain & Stucchi., 2005). To obtain the social license of all stakeholders, transparent monitoring and response methods must incorporate an in-depth comprehension of the natural systems to address public concerns. One way to achieve this is through prediction and monitoring of the effects of aquaculture wastes.

As with any other industry, aquaculture comes with waste products that must be studied to understand their effect on the environment. Since most marine systems replenish their waters with inputs from external sources such as river discharge, tides, and wind-based currents, it is important to ensure that release of waste products does not push the marine system beyond its ability to assimilate and remove said products without serious deleterious effects occurring. To protect aquaculture cage arrays from stress and damage caused by intense weather of the open ocean, they are often placed in sheltered bays. However, this placement comes with a price; these sheltered environments can have lower water renewal rates and water depths than that of the open ocean. Sufficiently low current velocities allow organic matter in the form of fish feces and excess food waste to sink beneath the cages, often forming a dense layer directly below and at differing radii beyond the cages (known as a depositional footprint) (Wildish et al., 2004; Strain & Hargrave, 2005; Giles, 2008). This organic matter can affect geochemistry and biodiversity of the sediment community on which it settles, principally due to changes in local oxygen demand due to decomposition (Hargrave et al., 2008). Determining the most effective means of assessing spatiotemporal gradients of organic loading can be difficult since numerous external variables create unique situations for each individual lease.

In Canadian finfish aquaculture, the accumulation of farm-origin organic matter and resulting oxygen demand are the framework around which monitoring programs are designed. Canadian monitoring assessment criteria are outlined in the Aquaculture Activities Regulations (AAR) documents, with deviations from outlined federal protocols existing at the provincial level to satisfy significant administrative and oceanographic variability between the provinces. Intensity of monitoring required is based upon site

specific characteristics such as lease size, modelled deposition contours, and historical geochemical observations. At the federal level, sites require bottom video footage, bathymetric surveys, and a primary focus on the monitoring of benthic geochemistry due to ease of acquisition and analysis (AAR, 2018; NSDFA, 2019a). In the absence of sufficient oxygen, sulfate can become the primary decomposition pathway for organic matter, resulting in the accumulation of dissolved sulfide byproducts, which can be toxic to benthic fauna at high enough concentrations. Because of this, determination of sulfide concentrations has been deemed as a suitable proxy for sediment health and adapted into a method for benthic monitoring that has been practiced at aquaculture farms for at least two decades (Wildish et al. 2001; Hargrave et al. 2008).

With a goal of environmental stewardship in mind, monitoring programs should act as a means of maintaining the current paradigm of the bay-scale ecosystem in which a resource exploitation resides. To do so, programs must be structured to promote sustainability, equity, and resiliency between linked systems (Soto et al. 2008). In Nova Scotia, monitoring of active sites normally occurs every year during the summer and early fall, with additional monitoring enforced if sulfide means at soft bottom sites are  $\geq 3000\mu\text{M}$ , with further mitigation strategies implemented if recovery does not occur (NSDFA, 2019b). At least two sample locations per cage array are taken from the cage edges, increasing in frequency by one for every 100,000 fish above 200,000, and at least one reference station located between 100-300m from the array edges. While the current monitoring program is valuable, the extensive variation in farm hosting environments makes it difficult to develop federal and provincial monitoring methods that effectively capture benthic responses that occur on different spatiotemporal scales. For example, only

taking samples from the edges of the cage array prevents the ability to determine size of the depositional footprint of the farm; unless waste dispersion by the water column between the cage array and receiving sediment is zero, waste will travel beyond the edges of the array, accumulating in unmonitored sediments. Additionally, factors such as hydrodynamics, sediment composition, historical culturing practices, and proximity to both the coastline and other ecosystem services can cause variability in response to organic loading at sites within the same bay.

Recent research posits that proactive, as opposed to reactive, methods of corporate sustainability management lead to better environmental performance (Kim, 2018), which can lead to increased corporate gains (Hart et al., 1996). An effective method for proactive site management could involve the utilization of a model that predicts benthic response to organic loading. In Canada, existing models for finfish aquaculture are currently relegated to only predicting waste deposition and have yet to be mandated for site management beyond initial site assessment and expansion (AAR, 2018; NSDFA, 2019b), meaning active sites can go years without any further modelling occurring. This leaves all proactive decisions to be informed by annual monitoring observations. Even the most advanced models cannot account for every variable, making predictions less accurate as changes from unaccounted for variables compound over time. Additionally, sulfide concentrations are not presently required for modelling regulations, despite sulfide analyses being fundamental to ongoing monitoring at active sites (NSDFA, 2019a; NSDFA, 2019b). Marine sediment sulfide concentrations have been previously modelled with varying levels of success (Paraska et al., 2014), indicating a potentially underutilized functionality of environmental monitoring.

I hypothesize that present monitoring practices are insufficiently capturing the variability of aquaculture site environments in bay-scale ecosystems, preventing adequately informed decision making. However, by combining new approaches to waste deposition and marine diagenesis into an ecosystem model, predictions of sediment sulfide distributions can be used to fill decision-making knowledge gaps. By collecting data beyond provincial and federal monitoring standard requirements, a precedent can be set for assessing whether the federal and provincial monitoring methods are sufficiently designed to be in line with a sustainable approach to aquaculture management.

### *1.1 Outline*

The present research has been divided into two sections that assess different aspects of aquaculture site monitoring and response to organic loading of aquaculture origin. Both sections involve the use of data from aquaculture leases in Shelburne, Nova Scotia, Canada.

- **Chapter 2** contains an analysis of both the available historical monitoring data for three sites within Shelburne Bay from 2004-2019, as well as a high-frequency sampling regime conducted at the same sites in 2019. Assessment of the historical monitoring dataset was used to explore the different responses to organic loading between sites and over time, whereas the high-frequency sampling dataset was used to determine if any meaningful patterns were present at different spatiotemporal scales than what was captured by the historical monitoring dataset.
- **Chapter 3** presents the development of a benthic diagenesis model, optimized to focus on the response to organic carbon loading and the resulting dissolved sulfide accumulation in the upper sediments. Results involve the response in variables of

concern due to changes in important parameters such as mineralisation rate and depositional flux composition. Model results were validated through comparison to historical monitoring data from two soft bottom lease sites.



## **CHAPTER 2**

### **COMPARATIVE ANALYSIS OF FINFISH AQUACULTURE SITES WITHIN SHELBURNE BAY, NOVA SCOTIA**

#### **2.1 Introduction**

Marine aquaculture depends on healthy functioning coastal ecosystems to provide suitable water/sediment quality and site locations. However, it is known to have a variety of potential environmental effects, including release of wastes such as dissolved nutrients, feces, and uneaten feed. Among these effects, there is emphasis on the benthos since sediments integrate environmental impacts with less short-term variation compared to the fluid water column. Deposition of particulate wastes to the bottom may cause eutrophication responses to organic loading including localized sediment hypoxia (Gray et al., 2002; Diaz & Rosenberg, 2008). Various sampling-based metrics and indicators are employed to document these effects and assess their deviation from 'normal' conditions. Faunal responses are often construed from the Pearson-Rosenberg (Pearson & Rosenberg, 1978) model of succession, in which small and numerous opportunistic faunas exploit organically enriched sediments. Because organic input causes excess bacterial metabolism and oxygen depletion, these measures include geochemical variables indicative of anaerobic processes, namely sulfate reduction. The end product of sulfate reduction is dissolved sulfide which can accumulate at high concentrations in sediments and interstitial waters.

An ecosystem approach to aquaculture (EAA; Soto et al., 2008) involves consideration of aquaculture influences beyond the local farm level, although there are few studies of far-field effects of fish farming. An important foundation for bridging potential

local and far-field effects is an understanding of the benthic footprints of waste originating from cages, including a comparison to surrounding reference sites. Factors such as bathymetry and 3D current structure can alter depositional pathways such that benthic footprints deviate from a mirror-image of the cage array.

In Canadian finfish aquaculture, accumulation of particulate organic matter (POM) from farms and net effects of benthic metabolism (oxic state) are the framework around which monitoring programs are designed. Canadian monitoring criteria are outlined in the Aquaculture Activities Regulations (AAR) documents (AAR, 2018), with some differences in practice existing at the provincial level. In Nova Scotia, site monitoring is conducted annually, with potential of increased sampling required if previous results indicate adverse effects, followed by site management mitigation strategies if effects persist. Other than historical data, required monitoring is based on site-specific characteristics such as lease size and predicted contours of POM using modelling tools such as DEPOMOD (Cromeey et al., 2002). At the federal level, sites require bottom video footage, bathymetric surveys, and benthic geochemical sampling with a focus on dissolved sulfide concentrations (AAR, 2018). The latter is used as a proxy for sediment health (Wildish et al. 2001; Hargrave et al., 2008) since the accumulation of sulfides is a key indicator of benthic hypoxia/anoxia.

In addition to the local farm response to organic inputs, temporal dynamics of fish production provide insight into benthic changes during fallow periods. Farms are required to allow time for benthic recovery between farming activity, which can manifest in cage rotation within the lease boundaries or complete site fallowing. Studies of fallowing frequently involve methods to quantify geochemical indicators and/or faunal community

structure. However, there are divergent findings regarding the time scales of recovery, with some reporting full recovery in 2-6 months (Ritz et al., 1989; Brooks et al., 2003; Brooks et al., 2004) while others reported periods of 1-6 years (Karakassis et al., 1999; Pereira et al., 2004; Macleod et al., 2008; Brooks et al., 2004; Keeley et al., 2014; Keeley et al., 2015), as well as differential recovery between the two indicator types (Pereira et al., 2004; Brooks et al., 2004; Lin & Bailey Brock, 2008; Aguado-Giménez et al., 2012). Biological indicators are more time and labour intensive than geochemical measurements, leading Canadian regulators to embrace the latter in monitoring programs.

While orientation to EAA can be achieved by comprehensive spatial sampling programs, these are labour and analysis-intensive. Spatially synoptic methods akin to remote sensing provide detailed coverage and greater resolution. Among these approaches, acoustic bottom signature remains poorly explored as a methodology in the context of environmental impacts. Previous studies have detected acoustic signatures associated with unconsolidated sediments at fish farm sites (Wildish et al., 2004). These signatures could be used to determine the extent of depositional footprints with greater resolution than is presently feasible. Nonetheless, a relationship between acoustic characteristics and geochemical measures of benthic health must be established.

In the present study, we undertook detailed temporal and spatial sediment sampling at two active salmon farms and one active trout farm in a large Nova Scotian bay. Sulfides and other benthic variables were measured at these locations and at reference sites as indicators of hypoxia. In addition, we analyzed historical records for the same variables on these farms dating back to 2004. Objectives were as follows:

- Use detailed spatial and seasonal sampling to document patterns of sediment sulfides and other variables around three active fish farm sites
- Undertake acoustic bottom surveys as an additional data layer for use in assessing benthic changes potentially due to fish farms
- Combine new spatial sampling and historical records to examine time scales of benthic response to farm activity and fallowing

## **2.2 Methods**

### *2.2.1 Study sites*

Sample sites were three fish farms on the South Shore of Nova Scotia in Shelburne Bay. The inner Shelburne Harbour contains an active fishing port and at the head is fed by the small Roseway River. Maximum depth of the harbour is 13m. Tidal range is 1.7m. Outer Shelburne Bay is exposed to open ocean and has a maximum depth of 16m. More recently, aquaculture studies of benthic conditions in Shelburne Bay have involved extensive bottom type characterisation through acoustic and benthic geochemical analysis, and assimilative capacity modelling (Bravo, 2017), as well as oceanographic conditions analyzed in conjunction with dissolved oxygen at the McNutts fish farm (Burke et al., 2021). Two sites were located toward inner Shelburne Harbour (Sandy Point, Hartz Point) and the third site was further seaward (McNutts) adjacent to McNutts Island (Figure 2.1). Stocking density, species, and cage array sizes differ between the three sites (Table 2.1). All three farms use barges to distribute feed to the cages.

In addition to the present study, data collected in 2004-2019 for the environmental monitoring program (EMP), developed and enforced by the Nova Scotia Department of

Fisheries and Aquaculture (NSDFA), was included in analysis to provide observations that had occurred at timeframes during previous culturing seasons that were not captured in the present study.

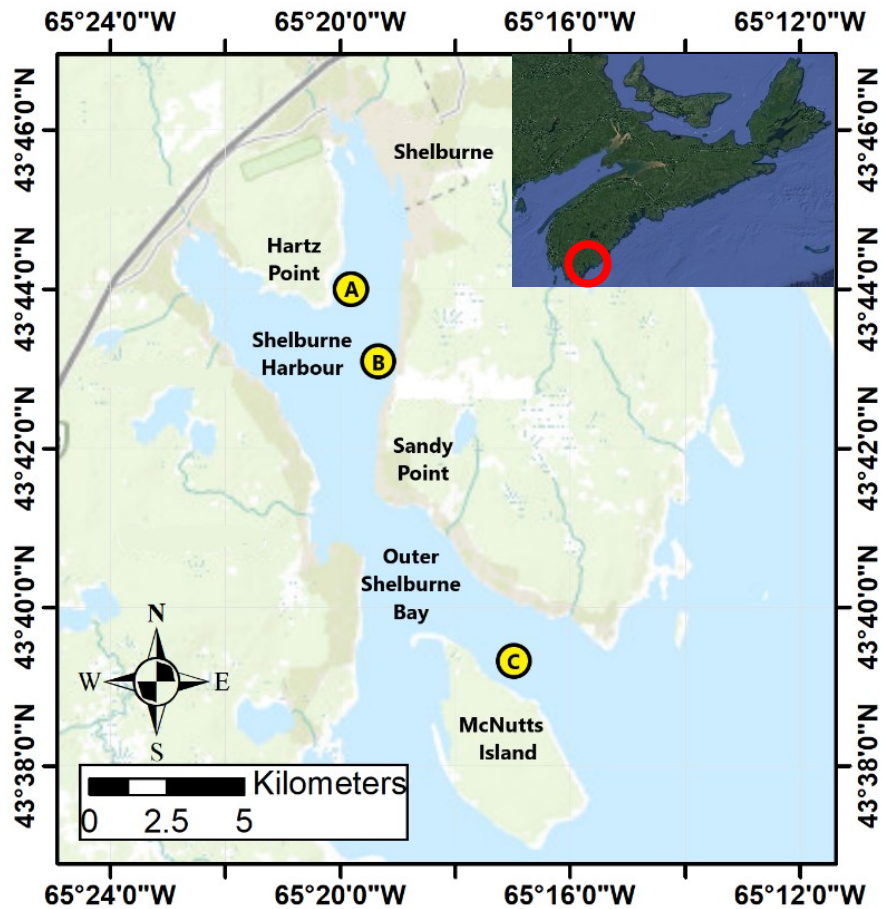


Figure. 2.1: Study site in Shelburne, Nova Scotia. Red circle = location of Shelburne in Nova Scotia; A = Hartz point lease; B = Sandy point lease; C = McNutts island lease.

Table 2.1: List of relevant parameters and variables for Hartz Point, Sandy Point, and McNutts lease locations

	<b>McNutts</b>	<b>Sandy</b>	<b>Hartz</b>
Species	Atlantic Salmon	Rainbow Trout	Atlantic Salmon
Status: 2014-2018	Stocked	Fallow	Fallow
Status: 2019-2020	Stocked	Stocked	Stocked
Active Cages	20	9	10
Grainsize Category	Sand	Mud	Mud
Stock Date: 2019	04/26	06/04	05/25
Time from last harvest (years)	0.28	>5	>5
Mean Smolt Size (g)	118	153	111

### 2.2.2 Field Methods

Sediment samples were collected at the three farm sites in July, August, October, and November 2019. Frequent high winds and currents relegated sampling locations to those on or near leases where tying off to buoys was possible, along with a few distant anchor points (Figure 2.2). Sediment samples were collected in duplicate at each location using a Petite Ponar Grab, with an opening of 15.2 x 15.2 cm. Removeable top screens were replaced with solid plate inserts to reduce disturbance of sample surface sediment during retrieval. Standing water was siphoned from the grab to ensure minimal disturbance of the sediment. Truncated plastic 5 ml syringes were used to retrieve the sediment samples from three points on the surface by inserting the syringe into the top 2 cm, gently withdrawing to avoid air bubbles in the sample and reinserting it twice more for a total ~5-6 ml of sample. The sample was then either transferred to a 20 ml scintillation vial for POM and water content analysis or remained capped in the syringe for dissolved sulfide and redox analysis. This procedure is in accordance with NSDFA protocols (NSDFA, 2019a)

which allows comparison to historical data. A trowel was used to collect subsamples for grain size analysis of volumes ~250 ml.

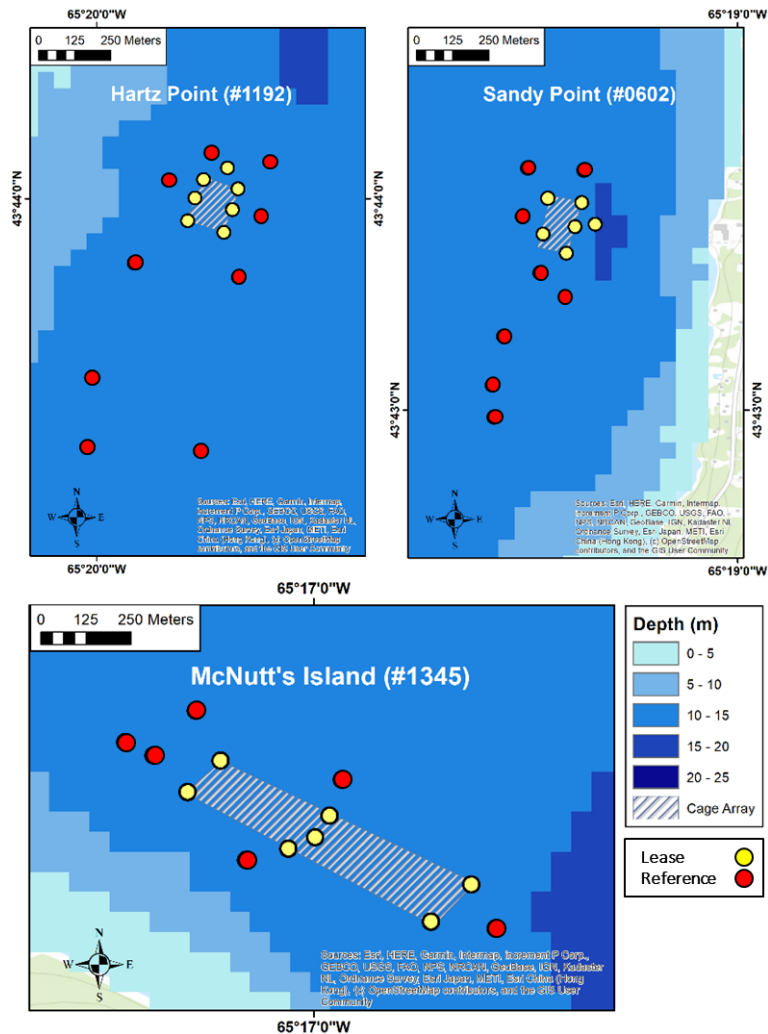


Figure 2.2: Sample locations for aquaculture lease sites in Shelburne Harbour and outer Shelburne Bay.

### 2.2.3 Acoustics

Acoustic readings were collected during August and October of 2019 using a BioSonics MX single beam echo-sounder, then imported to Biosonics Visual Habitat software for assessment. Boat speed did not exceed 5 knots while within the sampling area. The echo-sounder was set to 204.8 kHz with an 8.6° beam angle. Previous echo-sounding results collected in 2014 (Bravo, 2017) indicated that the sediments from which the

samples were taken were of similar types, but the transects used when collecting the data in 2014 were not as closely spaced as those collected during 2019. Gaps in transects appear when boat speed exceeded the 5 knots speed limit (Figure 2.3).

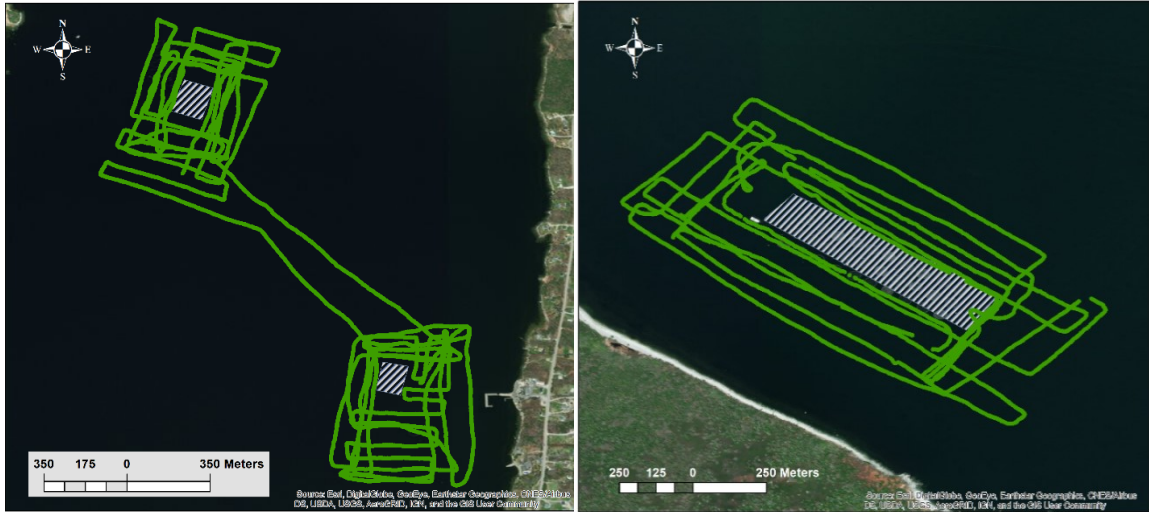


Figure 2.3: Echo-sounding transects from August and October of 2019 around all three sites.

#### 2.2.4 Laboratory Methods

Sediment samples were weighed wet ( $ww$ ), dried at  $60^{\circ}\text{C}$  for 24-48h, and dry weight ( $dw$ ) determined. Water content was then calculated as:

$$\text{Water Content} = \frac{(ww - dw)}{ww} \times 100\% \quad (\text{Eq. 2.1})$$

Aliquots of the dry samples were then transferred into pre-weighed tins, weighed, and combusted in a muffle furnace at  $490^{\circ}\text{C}$  for a minimum of 8 hours. After removal, tins were re-weighed to determine ashed weights ( $aw$ ), and POM content was calculated as:

$$\text{POM} = \frac{(dw - aw)}{dw} \times 100\% \quad (\text{Eq. 2.2})$$



Redox potential was measured using an Orion (96-78NWP) oxidation-reduction potential (ORP) platinum electrode, placed directly into the sediment sample, and recorded in millivolts. Temperature was also recorded to correct the redox potential relative to the normal hydrogen electrode ( $mV_{NHE}$ ):

$$mV_{NHE} = E_0 + (224 - T) \quad (\text{Eq. 2.3})$$

where  $E_0$  is the meter reading in mV and  $T$  is temperature in degrees Celsius. Twenty-four hours prior to analysis, the electrode was prepared and filled with 4M KCl filling solution. An electrode accuracy check was completed using an ORP standard (ORI967901) before and after all samples were analyzed, where the electrode was deemed accurate if the redox potential reading was  $+220\text{mv} \pm 3\text{mV}$  at  $25^\circ\text{C}$ .

Immediately following the measurement of redox potential, the sediment sample was measured for dissolved sulfide ( $\text{S}^{2-}$ ) concentration by first adding sulfide antioxidant buffer (SAOB) to create a slurry of equal parts sediment and SAOB. Increased pH converts  $\text{H}_2\text{S}$  and  $\text{HS}^-$  to  $\text{S}^{2-}$ , which is measurable by the electrode. The dissolved sulfide concentration was then measured using an Orion (96-16BNWP) Silver/Sulfide combination electrode placed directly into the sediment slurry. The dissolved sulfide concentration was later converted from mV to  $\mu\text{M}$  using a five-point standard curve created prior to analysis. To combat drift for the ISE probe, a new five-point standard curve was produced every 15 samples or every hour.

Grain size analyses were performed using the wet sieving method. Size bins were defined as  $\leq 63\mu\text{m}$ , 63-125  $\mu\text{m}$ , 125-250  $\mu\text{m}$ , 250-500  $\mu\text{m}$ , 500-1000  $\mu\text{m}$ , 1000-2000  $\mu\text{m}$ , and  $\geq 2000\mu\text{m}$ . All water that passed through the 63  $\mu\text{m}$  sieve was collected and a subsample filtered through a pre-weighed Whatman GF/F grade glass microfiber filter, which was

dried and weighed. Descriptive categorization and statistical analysis for further comparisons were determined using the Folk & Ward method (Folk & Ward, 1957).

### *2.2.5 Statistical Analysis*

Acoustic outputs were categorized using the fuzzy c-means clustering algorithm in Visual Habitat software. Visual Habitat allows the user to select any number of clusters to distribute acoustic signatures into, however there were no validation processes within the software, therefore four different methods for determining optimal number of clusters were utilized (Appendix, A.1). Once optimal number of clusters were determined, indicator kriging was used in Visual Habitat to interpolate the bottom-type distribution in the research area. Empirical variograms were divided into two sectors and oriented along the shorelines next to each farm. Semi-major axis lengths were set to 100-125m, to reflect distance between transects. Tension-method spline interpolation was used to generate maps for all sites on each sampling date. Interpolated values had greatest probability nearest to sample points and between sample points with high proximity. Acoustic bottom-typing is normally utilized to determine absolute sediment type; however, this research instead aimed to determine if the detrital footprint created a discernable signature within one absolute bottom type. Therefore, ground truthing through bottom video was not deemed necessary for this study. Instead, upon determination of optimal number of clusters, analysis of variance for mud content, water content, and organic matter was conducted between each cluster to determine if a combination of these variables were significantly responsible for differences in acoustic signatures.

Differences between group means of sediment geochemistry, acoustic bottom signatures, reference vs. lease locations, and sample date were assessed non-parametrically

using Kruskal-Wallis and Mann-Whitney U tests. All data from the present study was analyzed independently from the overlapping EMP data from 2019. In the EMP data, the number of samples taken at reference sites were frequently less than three, prompting an aggregation of reference samples into a single value for each site. Relationships between geochemical variables for each site across all years were tested using single linear, exponential, nonlinear exponential, and multiple-additive linear models, which were constructed with various log transformations for comparison to previously reported best-fit models and methods in Wildish et al. (1999) and Hargrave (2010). While relationships were measured for entire datasets, data was also constrained to redox potential values  $<0\text{mV}$  for sulfide comparison because of the other reactions that effect redox measurements  $>0\text{mV}$  (Whitfield, 1969). Model equations for redox potential and sulfides were compared to the nonlinear exponential model used in the development of a benthic enrichment nomogram currently utilized by the Nova Scotia EMP (Hargrave et al., 2008; Hargrave et al., 2010). Both residual standard error (RSE) and  $R^2$  values were provided for each model, though  $R^2$  values for nonlinear models are not considered a reliable method for measuring model suitability, with ANOVA used to compare models.

## **2.3 Results**

### *2.3.1 Sediment Geochemistry*

#### *2.3.1.1 Grain Size*

McNutts consistently displayed a sand textural group, with minimal differences between lease and reference sites in median diameter and sorting (Table 2.2). Mean mud content was generally 1-1.5% with a few values exceeding 2% (Figure 2.4A). Hartz and

Sandy study areas were either mud or sandy mud textural groups, with median diameter sizes ~35 times less than those of McNutts at 10-12 $\mu$ m, and relatively poor sorting. Sediments at Hartz Point were dominated by mud on all sampling dates with a range from 66 to 96% over the whole data set (Figure 2.5A). Sediments at Sandy Point were similar to Hartz Point, again dominated by mud on all sampling dates with a range from 30 to 97% over the whole data set (Figure 2.6A), and no obvious difference between lease and reference sites. However, Sandy was also characterized by irregularities in sediment texture, with occasional large stones and/or shells. Comparisons of lease and reference sites at Hartz and Sandy produced only minimal differences for both median diameter and sorting.

Table 2.2: Mean grainsizing results for lease and reference study areas.

<b>Grain Sizing</b>				
<b>Site</b>	<b>Location</b>	<b>Textural Group</b>	<b>Median Diameter (<math>\mu</math>m)</b>	<b>Sorting (<math>\mu</math>m)</b>
McNutt's	Reference	Sand	344.4	1.8
	Lease	Sand	359.8	1.9
Hartz	Reference	Sandy Mud	10.3	5.3
	Lease	Mud	9.9	5.1
Sandy	Reference	Sandy Mud	10.7	5.7
	Lease	Sandy Mud	12.3	7.2

### 2.3.1.2 Spatiotemporal Patterns: Present Study

#### *McNutt's*

Mean water content was consistently 22-23%, with changes to monthly lease means paralleling those of mud content (Figure 2.4B). Differences between lease and reference values never exceeded 0.5. Organic content was characteristically low, typical of coarse sediments, with mean values <0.6 wt.% and maxima of 1 wt.% (Figure 2.4C). Again,

changes to monthly means from the lease followed the same pattern present for both water content and mud content. Differences between lease and reference values were all  $\leq 0.3$  wt.%. When notably high values were measured, they were found to be either at the southwestern or southeastern edges of the cage array, the feeding barge to the northwest, or a combination of the three.

Though POM content was low throughout the sampling period, any relatively high organic content values frequently aligned with increased sulfide and lower redox values. Redox was uniformly positive with means  $>100\text{mV}$  as expected in sandy aerobic sediments, and differences between lease and reference means were  $<30\text{mV}$  (Figure 2.4D). Consequently, sulfides were low with means  $<100\mu\text{M}$ , although an individual replicate reached  $450\mu\text{M}$  (Figure 2.4E). Given the consistency of these results and low range of values for variables such as sulfide, there were no apparent differences between sampling dates or lease/reference sites.

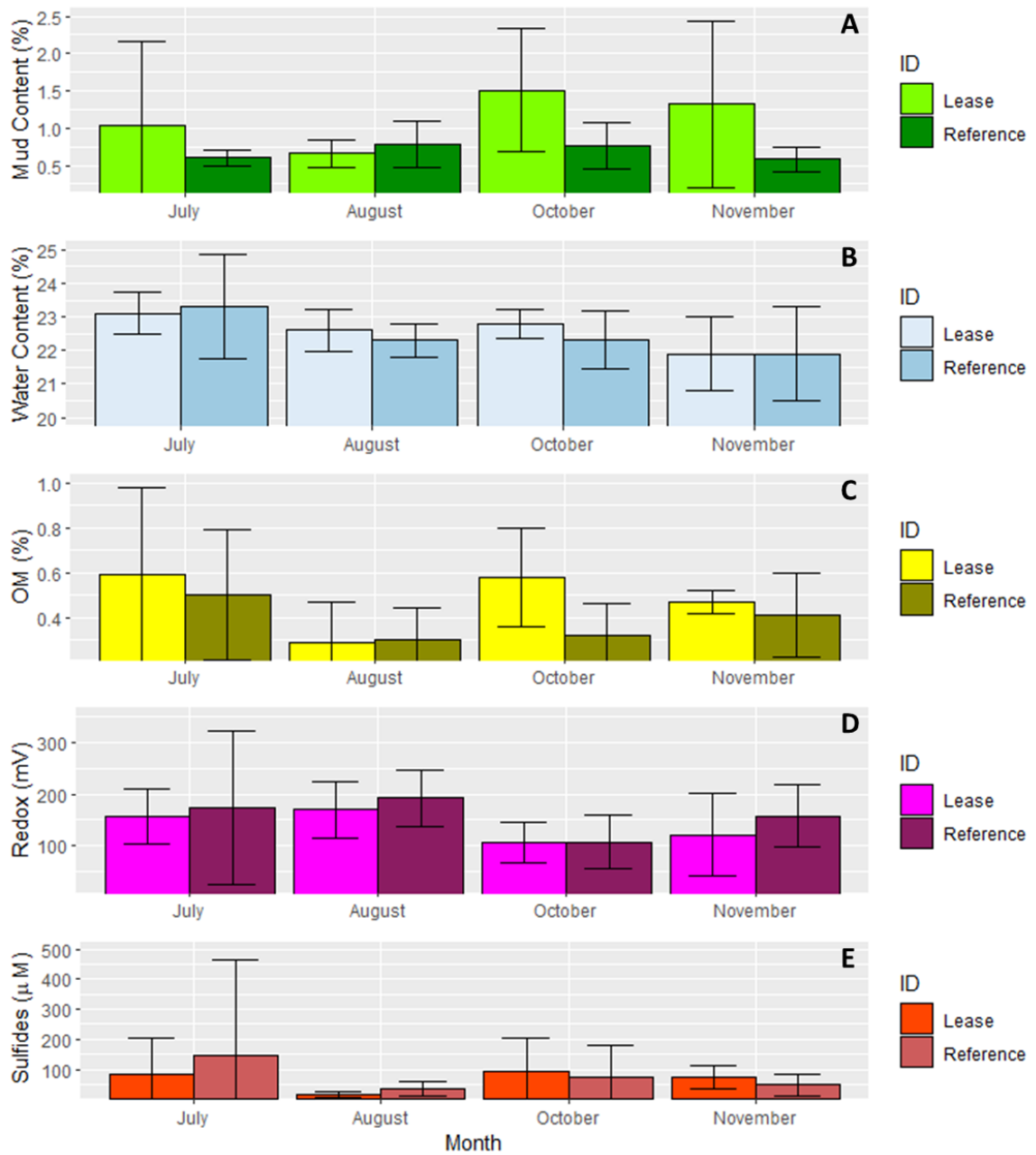


Figure 2.4: Geochemical variable results for July, August, October, and November 2019 at the McNutts Island site. A = Mud content (%), B = Water content (%), C = Organic Content (%), D = Redox potential (mV), E = Dissolved sulfides concentration ( $\mu\text{M}$ ). Bars represent mean and stems represent standard deviation.

## *Hartz*

As expected of muddy sediments, water content was uniformly high with means of 78-82% and little variation over time or among sampling sites (Figure 2.5B). Consistent with porous, muddy sediments, organic content was high with a range in individual samples of 11-22 wt.%. Mean values were mostly 16-17 wt.%, except in August which had lease and reference means of 19 wt.% (Figure 2.5C). There was no apparent difference between reference and lease sites. Redox values were mostly positive but with means always <100mV (Figure 2.5D). Mean negative values occurred only at the lease site in October and November with minima in individual replicates of -128mV. Both lease and reference means followed a decreasing trend from July to November, though the decreases of the reference values were notably less than those of the lease. Of the four months, both October and November had significantly lower redox values at the lease compared to reference values. Sulfide was surprisingly low for depositional muds with all lease means <750 $\mu$ M, and reference means <200 $\mu$ M (Figure 2.5E). However, individual replicates at the lease sites had sulfides as high as 1800-3000 $\mu$ M in October and November. November was the only month that showed significantly higher sulfides at the lease compared to reference values. Maximum or near maximum sulfide and redox values were always located on cage array corners, however, corners with higher values were inconsistent across months, with previously high value sample locations recovering between sampling dates.

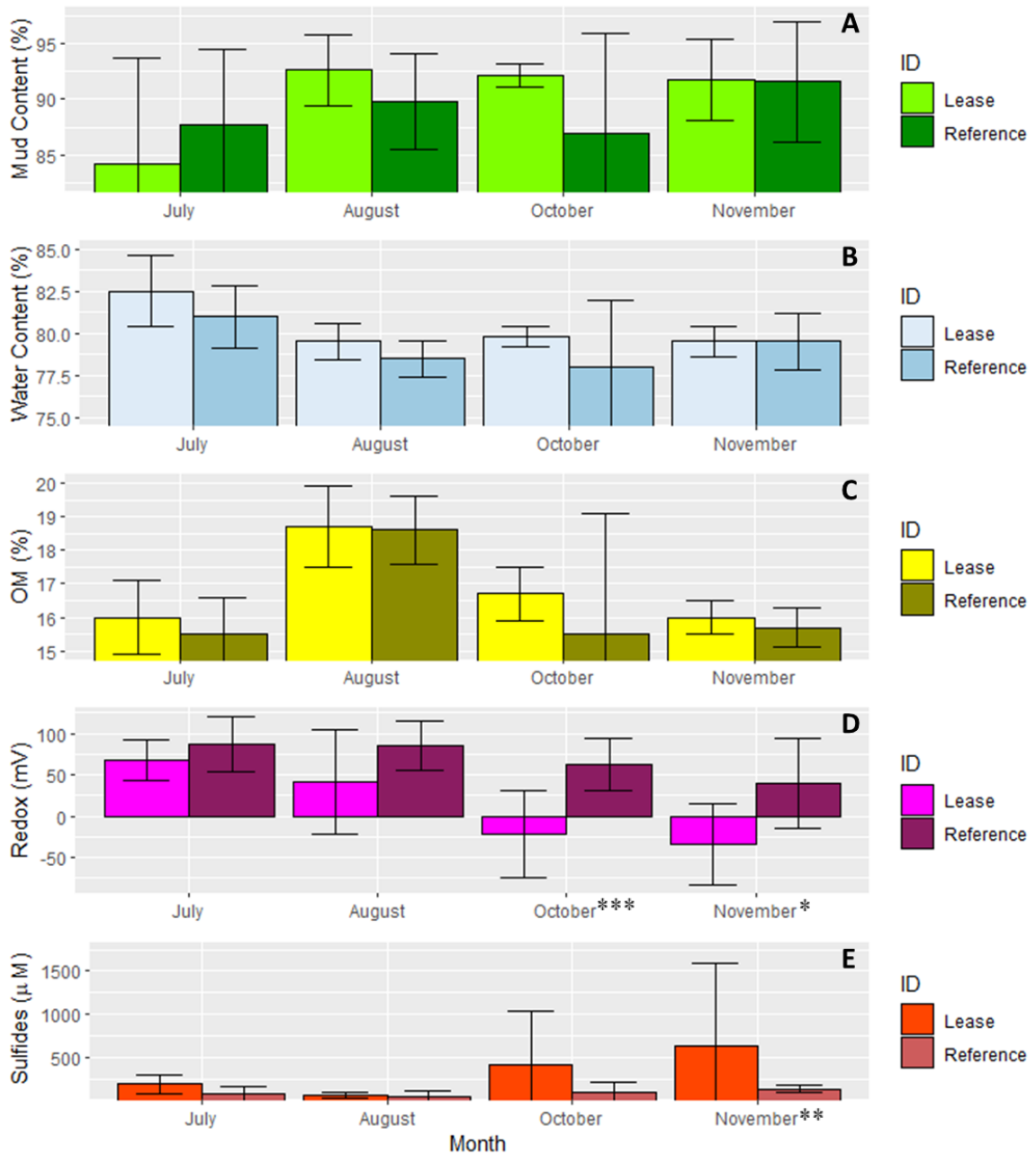


Figure 2.5: Geochemical variable results for July, August, October, and November 2019 at the Hartz Point site. A = Mud content (%), B = Water content (%), C = Organic Content (%), D = Redox potential (mV), E = Dissolved sulfides concentration ( $\mu\text{M}$ ). Bars represent mean and stems represent standard deviation. P-value:  $0.01 < * \leq 0.05$ ,  $0.001 < ** \leq 0.01$ ,  $*** \leq 0.001$ .



### *Sandy*

Water content was uniformly high with means of 73-78% showing changes of 2-4 units between sampling dates at the lease, and little difference between months after a decrease in August at reference sites (Figure 2.6B). Organic content was lower than Hartz, but still quite high with a range in individual samples of 5-16 wt.% (Figure 2.6C). Mean values ranged from 12-15 wt.%, increasing from July to October before dropping to the lowest point in November for lease values, and reference sites were all within 1 wt.% of each other except for a relatively high 15 wt.% mean in August. Lease redox values were mostly positive with means ranging from 25mV to -50mV, showing a consistent downward trend from July to November (Figure 2.6D). Mean negative values occurred only at the lease site from August to November with a minimum in individual replicates of -167mV. Reference means followed a decreasing trend from July to October, with a negative value in October before increasing in November to 0mV. Sulfide was again low, but monthly means were cumulatively greater than those found at Hartz. All lease and reference means were <750 $\mu$ M, while reference means in July and August were <200 $\mu$ M (Figure 2.6E). Higher reference site values were measured in October at 900-1500  $\mu$ M, producing a value larger than the October lease mean of >500 $\mu$ M. An individual replicate at the lease site in August had sulfides of 2500 $\mu$ M, whereas the next highest measurement was 850  $\mu$ M. Relatively high sulfide and low redox values were initially situated on the northeastern corner of the cage array in July and August, however in October and November most locations, both on and off the lease, had similar results. None of the variables showed significant differences between lease and reference sites for any of the sampling dates due to high variability.

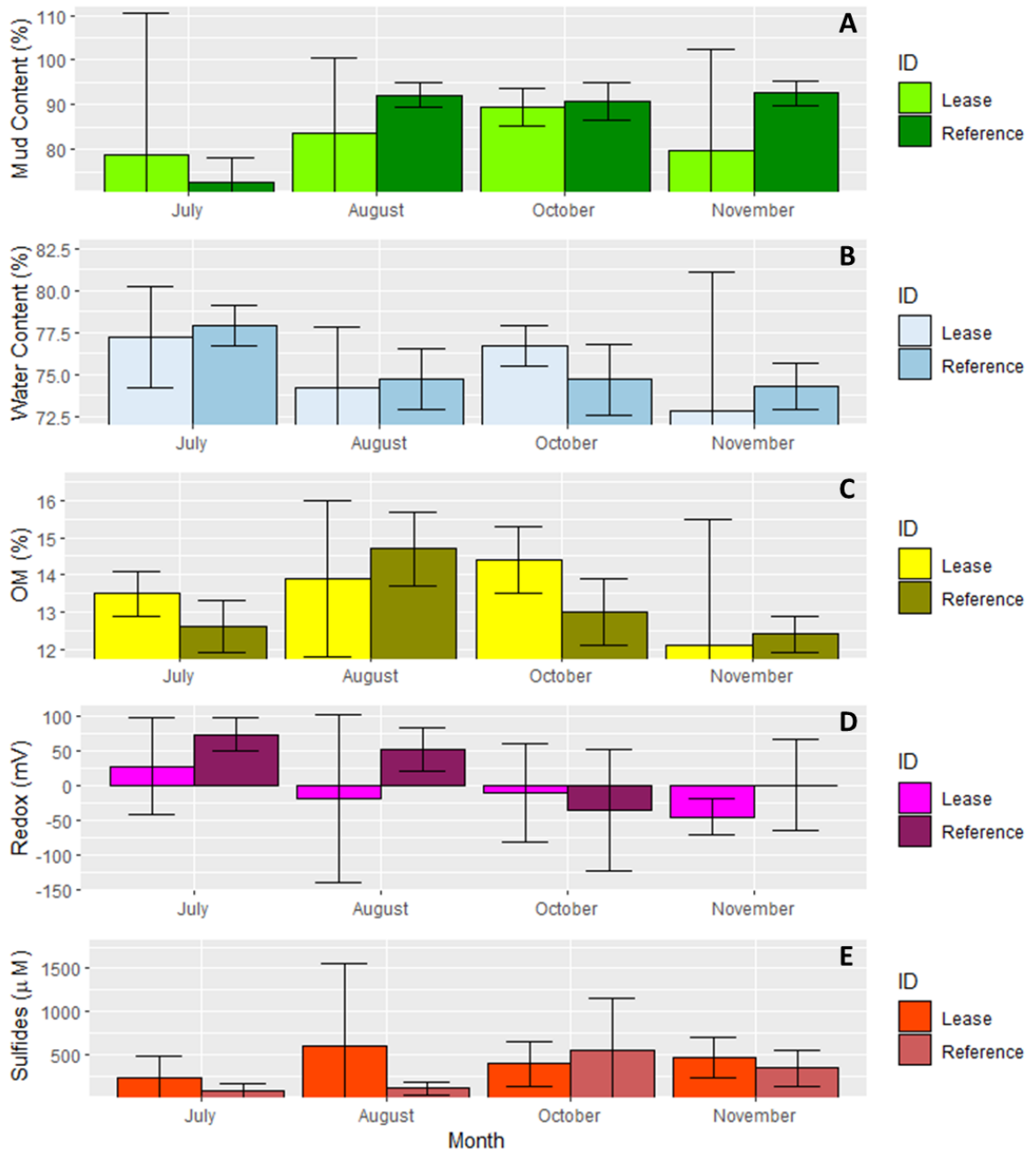


Figure 2.6: Geochemical variable results for July, August, October, and November 2019 at the Sandy Point site. A = Mud content (%), B = Water content (%), C = Organic Content (%), D = Redox potential (mV), E = Dissolved sulfides concentration ( $\mu\text{M}$ ). Bars represent mean and stems represent standard deviation.

### *2.3.1.3 Spatiotemporal Patterns: Historical Monitoring Data*

Due to the availability of provincial monitoring data via the Environmental Monitoring Program of the NS Department of Fisheries and Aquaculture, a retrospective analysis of sediment variables was undertaken. Comparisons between measurements of lease and reference values for each historical sampling year and the present research were used to determine if variations in geochemical measurements fell between or beyond confines of historical reference sites. Comparisons were completed through separate aggregations of lease and reference values from the present study, an aggregation of EMP reference values, and each set of annual lease values from EMP data. If present research values were between the confines of reference site historical variability, an inference of low or no influence from farm biodeposits could be made.

#### *McNutts*

Comprehensive provincial environmental monitoring and farming activity began at McNutts in 2010 and continues to the present. One of the major differentiating characteristics of McNutts from Sandy and Hartz was the consistent fish culturing during every year of operation and monitoring, restricting insight into extended fallowing beyond the typical 4-6 months following a 1.5 year production cycle. While most historical values for mean water content (18-21%) were lower than those measured in the present study, 2014 and 2018 both displayed higher values of  $25 \pm 7.6\%$  and  $30 \pm 11\%$ , respectively (Figure 2.7A). Individual measurements ranged from 14-49%, with 2014 and 2018 also having greatest variability amongst sampling dates. Measurements for lease and reference sites in the present study were significantly greater than those in EMP data from 2013, 2015 and 2019 (Table 2.3). Additionally, present study lease values were greater than EMP

reference values ( $p = 0.0189$ ), while no differences were present between EMP reference and lease values throughout (Table 2.4).

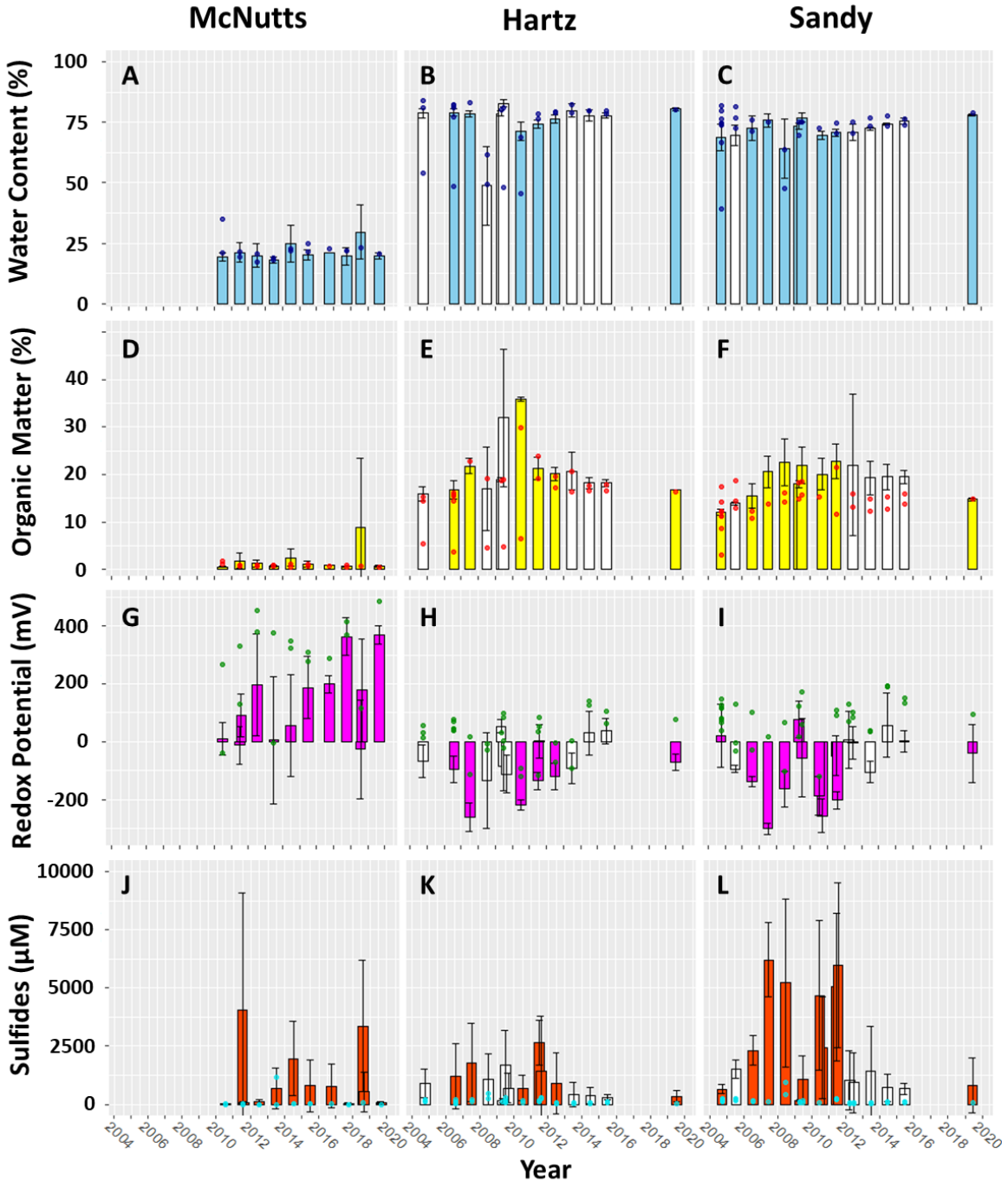
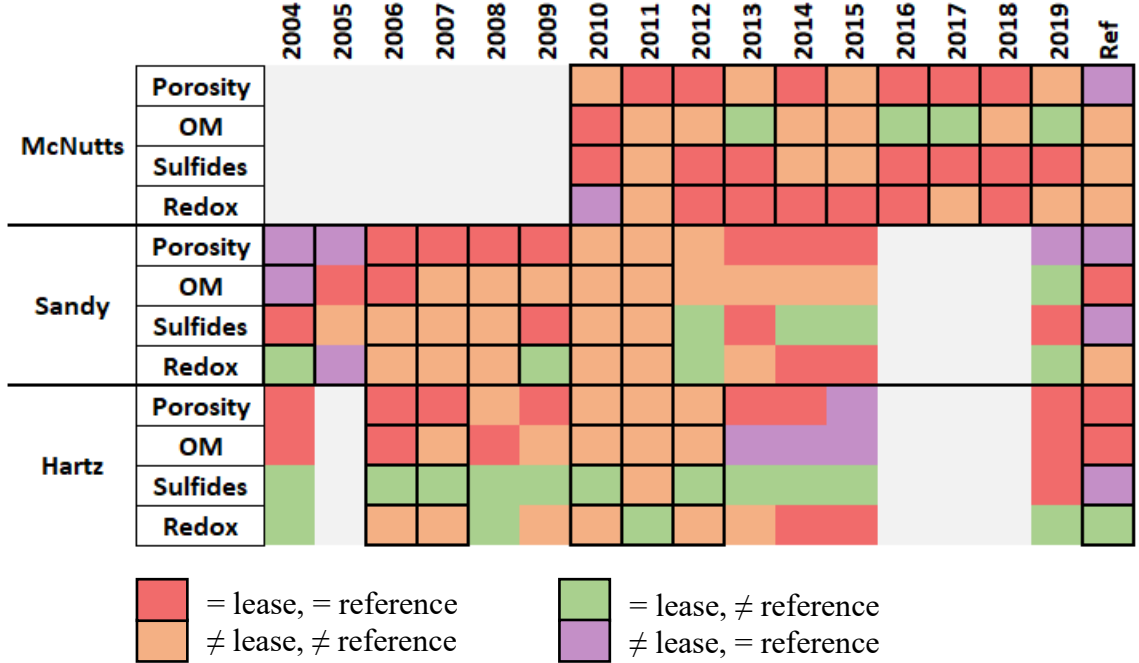


Figure 2.7: Historical geochemical variable results for McNutts, Hartz, and Sandy. A-C = Water content (%), D-F = Organic content (%), G-I = Redox potential (mV), J-L = Dissolved sulfide concentration ( $\mu\text{M}$ ). Bars = mean (coloured bars = fish presence, white bars = fish absence), stems = standard deviation, points = reference sites.

Table 2.3: Kruskal-Wallis comparison between present study and EMP data. Columns represent a total of all lease samples taken for individual years, plus the aggregate of all reference values. Bolded sections represent years where fish were present during monitoring. Benjamini & Hochberg (1995) p-adjustment method.

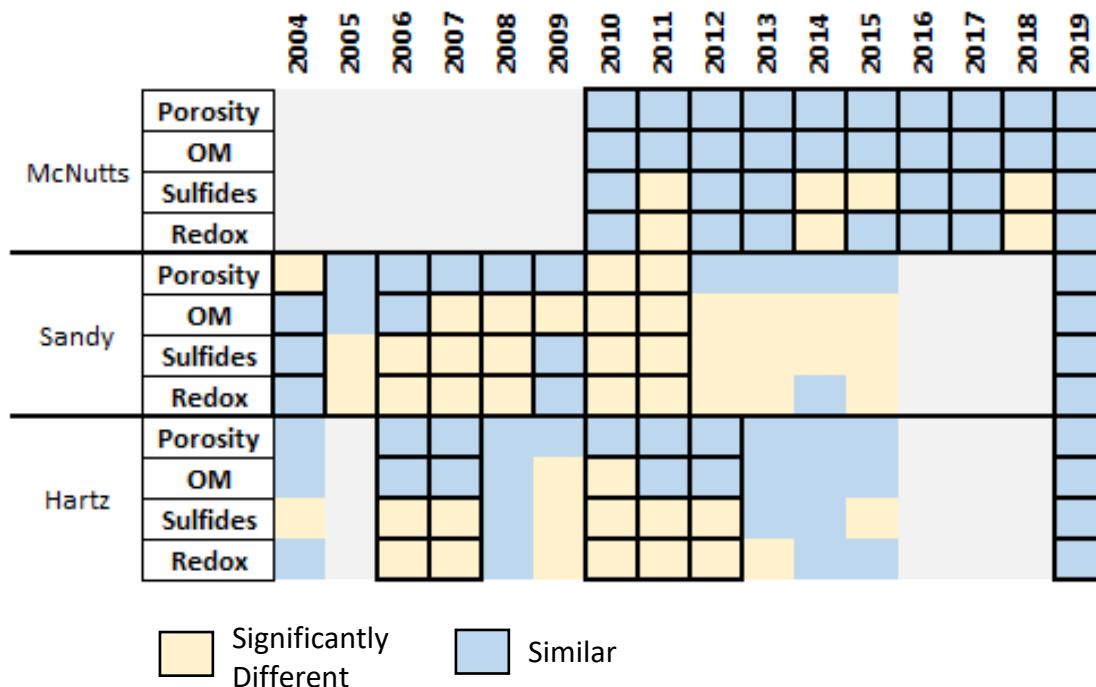


In contrast, organic content means of EMP values (0.6-8.9 wt.%) were greater than those in the present study in all years except 2010 (Figure 2.7D). Individual EMP samples ranged from 0.4-37.7 wt.%, with 2018 again registering the highest mean and greatest variability between years ( $8.9 \pm 14.5\%$ ). When comparing EMP data to the present study, significant differences in POM were more frequent than for water content (Table 2.3). Present reference values were significantly lower than EMP lease values from 2011-2019, with present lease values also significantly lower in 2011-2012, 2014-2015, and 2018. This pattern continued for comparison to EMP reference values, where both present study lease and reference values were significantly lower ( $p = 0.0001$ ;  $0.0002$ ). As with water content, no significant differences were present between EMP references and lease values throughout (Table 2.4).

Redox potential of EMP samples were mostly positive, with means ranging from -27–200mV and individual samples from -160-435mV (Figure 2.7G). Redox was consistently the most variable geochemical property, with high standard deviation and drastic changes between consecutive sampling dates. Both present study lease and reference values were significantly greater than EMP lease values in 2011, and significantly less than values in 2017, 2019, and EMP references (Table 2.3). EMP lease values were significantly lower than reference values in 2011, 2014, and 2018 (Table 2.4).

Most mean sulfides for EMP observations were much higher than the present study, with ranges from 10-2000 $\mu$ M and individual samples from 0-12000 $\mu$ M (Figure 2.7J). Secondary sampling was mandated at McNutts in 2011 and 2018, one month after initial sampling for each year, and though the secondary sampling locations were not exact in their successive retrieval, they were in close proximity. Secondary sampling values revealed a reduction in mean sulfides by 2000-3500 $\mu$ M and an increase in mean redox potentials by 100-200mV, all while culturing practices would not have deviated from normalcy. Both present study lease and reference values were significantly less than EMP lease values from 2011, 2014, and 2015, while also being significantly greater than EMP references (Table 2.3). EMP lease values had large standard deviations and were significantly greater than references at the site in 2011, 2014, and 2018 (Table 2.4). These high sulfide values were accompanied by relatively low redox and high organic content measurements.

Table 2.4: Kruskal-Wallis comparison of EMP data between the aggregate of reference values and total of all lease samples taken for individual years. Bolded sections represent years where fish were present during monitoring. Benjamini & Hochberg (1995) p-adjustment method.



*Hartz*

EMP monitoring at Hartz began in 2004, with extended fallowing beginning in 2013 and monitoring pausing in 2015, followed by a return to farming and monitoring activity in 2019. Most mean water content values in the EMP data were similar to those in the present study ranging from 56-83%, with individual samples ranging from 21-84% (Figure 2.7B). Most mean values were >75%, however a notably large decrease occurred in July of 2008 ( $49 \pm 16\%$ ), followed by the highest difference in values between dates in August 2009 ( $83 \pm 1.4\%$ ), and subsequently declining to values of 75-80%. Present study lease and reference values were significantly higher than EMP lease values in 2008 and 2010-2012 (Table 2.3). There were no significant differences between EMP references and lease values throughout (Table 2.4).

Mean organic content in the EMP data was mostly higher than values in the present study ranging from 17-32 wt.%, with individual samples ranging from 1-53 wt.% (Figure 2.7E). Monitoring results followed a positive trend of increasing POM from 2004-2009, before trending downwards from 2009-2019. The increase in 2008 ( $17 \pm 8.8\%$ ) to July 2009 ( $32 \pm 14\%$ ) was unexpected as fish were not present at the site during for both years. Present study lease and reference sites were significantly less than EMP values from 2009-2012 (Table 2.3). However, after this point in time, site values began to drop, leaving present lease values significantly lower from 2013-2015, but this was no longer the case for present reference sites compared to that time period. EMP lease values were significantly greater than reference values from 2009-2010 (Table 2.4).

Mean redox EMP values were highly variable between years ranging from -260-50mV, with individual measurements ranging -330-120mV (Figure 2.7H). Temporal patterns followed a negative trend from 2004 to 2007, a mostly positive trend from 2007 to 2015, then declined again in 2019. The large increase in organic content measured in 2009 was not reflected in comparatively lower redox to adjacent sampling years. Present reference values were significantly greater than EMP lease values from 2004-2013, 2019, and EMP references (Table 2.3). Present lease values favoured more to the lower end but were still significantly greater than EMP values in 2006-2007, 2009-2010, and 2012-2013. Redox potential of EMP lease values were significantly higher than reference values from 2006-2007 and 2009-2013 (Table 2.4).

Mean sulfide values from the Hartz EMP data were mostly higher than in the present study ranging from 300-2600 $\mu$ M, with individual samples ranging 10-7100 $\mu$ M (Figure 2.7K). A positive trend was observed from 2004-2011, with a brief decline in 2009-



2010, followed by a negative trend from 2011-2019. The notably low sulfide values found throughout 2009 ( $671 \pm 908\mu\text{M}$ ) were paired with an increase in redox potential ( $-36 \pm 91\text{mV}$ ), and unexpectedly high POM ( $23 \pm 12\%$ ). Most lease values for sulfide in the present study were not significantly different from EMP monitoring, with the exception of 2011 ( $p=0.0113$ ; Table 2.3). However, present reference values were significantly lower for nearly all years monitored, from 2004-2015. EMP lease values showed a similar pattern to redox potential, where significantly higher values compared to references were observed in 2004-2007, 2009-2012, and 2015 (Table 2.4). While higher sulfide values were observed on the lease in 2008 ( $1075 \pm 1080\mu\text{M}$ ), multiple low values were also observed, pushing the values towards similarity to the reference sites.

### *Sandy*

Similar to Hartz, Sandy also initiated provincial monitoring in 2004, and in 2012 followed for eight years, before activity and monitoring were resumed in 2019. Mean water content values were similar to those in the present study ranging from 64-78%, with individual samples ranging 52-79% (Figure 2.7C). Lower values were found in the early and middle years of monitoring. The same notable patterns seen in Hartz from 2008 onwards were also present at Sandy; with a large drop in 2008 ( $64 \pm 12\%$ ), an increase to highest mean value in 2009 ( $77 \pm 1.8\%$ ), and then a drop again in 2010 ( $70 \pm 1.8\%$ ) followed by a steady positive trend onwards. Present study lease and reference values were significantly greater than EMP lease values from 2010-2012 (Table 2.3). Additionally, present study lease values skewed towards higher values than present reference observations, making present lease values significantly higher than 2004-2005 and EMP

references, but lower than 2019 values. Between EMP lease and reference observations, lease values were significantly lower in 2004 and 2010-2011 (Table 2.4).

Most values for organic content in the EMP data were greater than in the present study, ranging from 14-21 wt.%, with individual samples ranging 12-59 wt.% (Figure 2.7F). A positive trend was seen from 2004-2009, followed by a consistent downward trend from 2011-2019. From 2007-2015, both present study lease and reference values were significantly lower compared to EMP lease values (Table 2.3). During those same years, EMP lease values were significantly lower compared to reference values (Table 2.4). However, present study reference values expectedly skewed lower than lease values, making them similar to EMP lease values from 2004-2006 but significantly lower than 2019.

Similar to the present research, mean redox for EMP data were mostly negative though to a greater degree, ranging from -300-60mV, with individual samples ranging -320-230mV (Figure 2.7I). Temporal trends followed a pattern similar to Hartz, decreasing from 2004-2007, increasing until 2009, a decrease in 2010, followed by increasing values onwards. Though still diverse, redox values for individual years had larger ranges at Sandy than Hartz, yet significant differences between present study and EMP values were still just as common. In 2004, 2006-2013, and 2019, reference values in the present study were significantly greater than EMP lease values, whereas present study lease observations skewed towards lower values, making them significantly similar to 2004, 2010, 2012, and 2019 (Table 2.3). Both present study lease and reference values were significantly lower than the EMP reference values. Nearly all years showed significantly lower lease to reference values between EMP data, with exceptions in 2004, 2009, and 2014 (Table 2.4).

Mean sulfides in the EMP data were almost always greater than the other two research sites ranging from 640-6200 $\mu$ M, with individual samples ranging 50-12000 $\mu$ M (Figure 2.7L). Temporal patterns showed a close inverse relationship with redox values with a positive trend from 2004-2007, decreasing to 2009, an increase until 2011, followed by a decrease until 2019. Present study reference values were significantly lower than EMP lease values from 2005-2008, 2010-2012, and 2014-2015 (Table 2.3). With slightly higher values, present study lease observations were only significantly lower from 2005-2008 and 2010-2011. EMP lease values also followed a similar comparison pattern to redox potential, where nearly all years were significantly greater than reference values except 2004 and 2009 (Table 2.4). Much like the redox comparisons, differences in sulfides between reference and lease sites were strong from 2005-2011.

### *2.3.2 Geochemical Correlations*

Relationships between sulfides and redox potential were the only one significant among the five variables measured at each site. However, the strength of these relationships and the best fit/most appropriate models for each site were different (Figure 2.8), though the nonlinear exponential models were universally a better fit than the linear model for all sites ( $p < 0.001$ ). When measuring relationships for the entire dataset for each study site, nonlinear exponential models had the lowest RSE and  $R^2$  values, however these curves produced asymptotes for the models  $> -200\text{mV}$ , a value where sulfides can still be one of the primary byproducts of metabolism (Table 2.5). Linear models with log transformed sulfides were only marginally worse in regard to RSE and  $R^2$ , and these models included  $\leq -200\text{mV}$  values. Relationships were found to be strongest at Sandy, which had the greatest frequency of low redox and high sulfide measurements. The models with the

lowest RSE were found to be nonlinear exponential models from the constrained <0mV datasets. For this model, RSE was ~50mV for Sandy and McNutts, and ~60mV at Hartz. McNutts showed the strongest relationship to the model proposed by Hargrave (2010) in both full and constrained datasets. Most values at both Sandy and Hartz fell below the Hargrave model curve, with values at Sandy fitting better at <0mV.

Table 2.5: Empirical relationship equations between dissolved sulfides vs. redox potential for 2004-2019. Nomogram f(x) RSE is in reference to the empirical relationship equation from Hargrave et al. (2010). P-value is the result of comparison of linear to nonlinear models using ANOVA.

Site	Function	Dataset	Formula	RSE (mV)	Nomogram f(x) RSE	DOF	R <sup>2</sup>	p-value
Sandy	Nonlinear Exponential	<0 mV	$y = 144 + 163 * \exp(-x/3147)$	48.59	161.4	94	0.5045	<0.001
	Linear	Full	$y = 152 + 287 * \exp(-x/1173)$	72.94	568.4	191	0.6647	<0.001
			$y = 703 - 63 * \ln(x)$	73.49			0.6561	
Hartz	Nonlinear Exponential	<0 mV	$y = 176 + 127 * \exp(-x/1110)$	62.17	100.5	68	0.4419	<0.001
	Linear	Full	$y = 183 + 246 * \exp(-x/550)$	66.25	637.0	143	0.5547	<0.001
			$y = 610 - 52 * \ln(x)$	69.1			0.5090	
McNutts	Nonlinear Exponential	<0 mV	$y = 228 + 83 * \exp(-x/2499)$	52.82	80.1	18	0.8778	<0.001
	Linear	Full	$y = 299 + 307 * \exp(-x/338)$	109.2	353.7	118	0.5060	<0.001
			$y = 691 - 45 * \ln(x)$	110.4			0.4868	

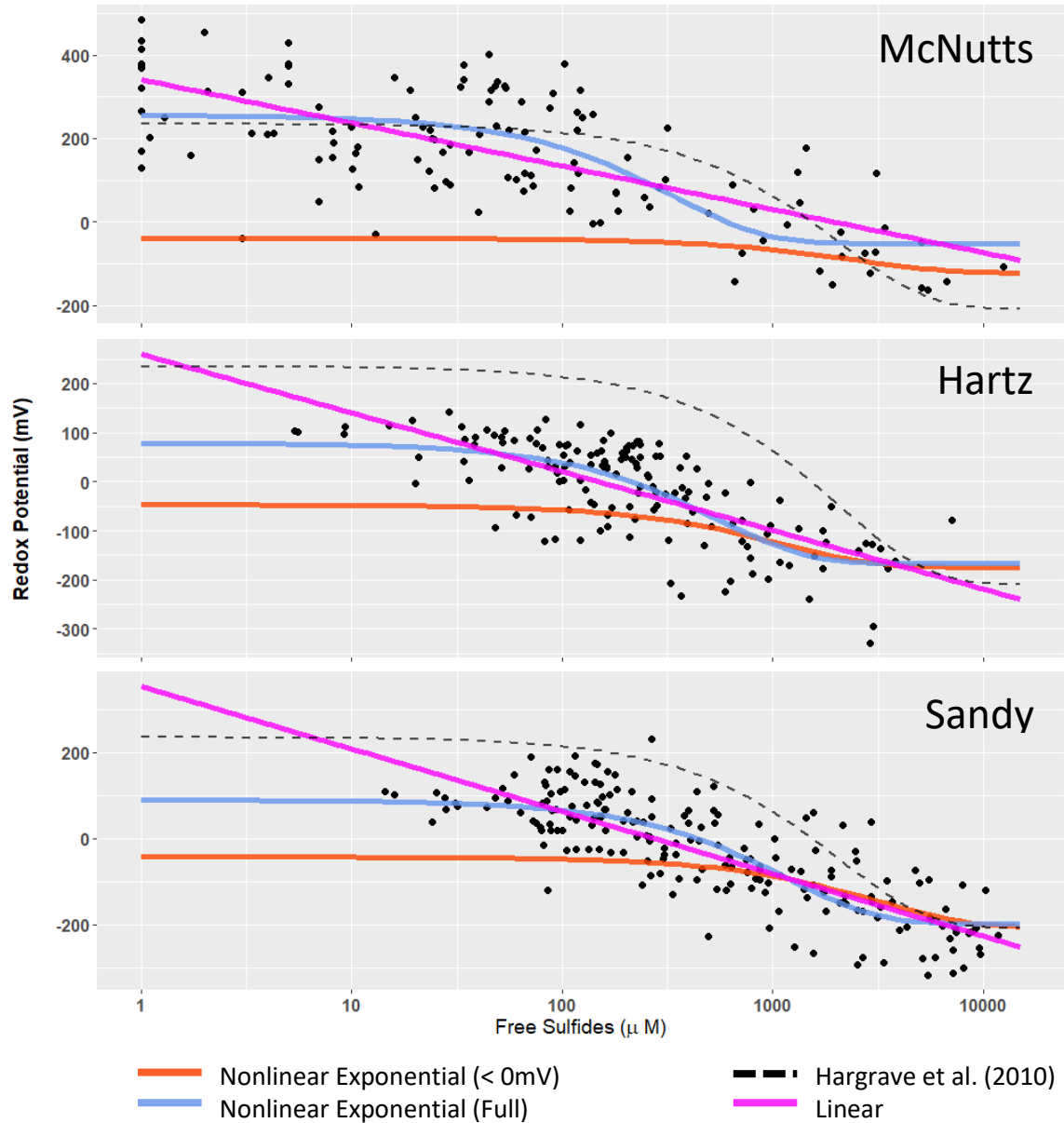


Figure 2.8: Empirical relationships between dissolved sulfides vs. redox potential for 2004-2019, separated by individual lease. Model equations described in Table 2.5.

### *2.3.3 Acoustic Bottom Signatures*

Acoustic data collected in August was less variable and more robust than that of October. Variogram ranges were around 100m for August and <20m for October, with errors  $\sim 8e-07$  and  $3e-06$ , respectively. Clustering of bottom signatures indicated that two clusters were the optimal categorization method across all sites for both August and October data collection (Figure 2.9), but these clusters were not identical across sites. Bottom Type B at Sandy and Hartz, and Type D at McNutts, consistently appeared less frequently than corresponding signatures at their respective study areas. This resulted in insufficient samples for comparison of bottom signatures in August at Sandy and McNutts. Mann-Whitney U tests between geochemical variables and the two bottom signatures at each site produced no meaningful relationships for all sites in October. However, significant differences were found for dissolved sulfide values at Hartz in August.

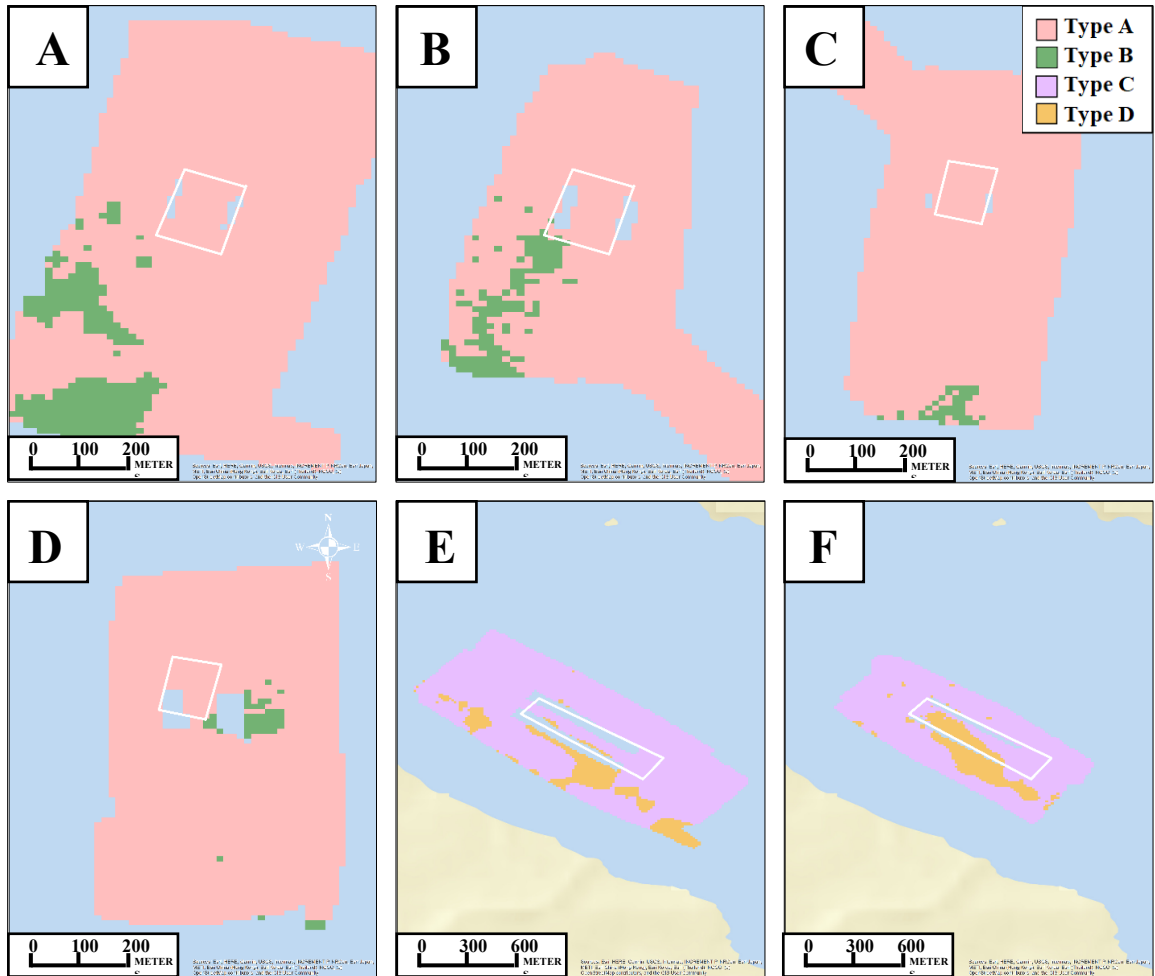


Figure 2.9: Kriging bottom type results for all three sites. A: Hartz – August, B: Hartz – October, C: Sandy – August, D: Sandy – October, E: McNutts – August, F: McNutts – October; blue area = no data.

## 2.4 Discussion

### 2.4.1 Spatial and temporal variability

With its larger grain size, McNutts exhibited a benthic system dominated by advective transport, whereas Sandy and Hartz were both more quiescent finer sediments. Sandier grain size corresponds to higher permeability (Masch & Denny, 1966), providing a higher rate of access to oxidants needed for POM mineralisation, and also higher rates of release and dilution of potentially toxic sulfides (Webster & Taylor, 1992; Boudreau et al., 2001). Relatively high macrofaunal abundance and resistance to organic enrichment from fish farms have been observed at high flow sites compared to neighbouring low flow sites (Keeley et al., 2013). These factors allowed McNutts to host nearly twice as many cages, each with similar biomass per cage as Sandy and Hartz, yet on average POM and sulfides were lower and redox potential was higher. Though comparisons of McNutts to the other sites produced the greater contrast, differences in benthic response between Sandy and Hartz were also observed.

For the high frequency sampling regime of the present study, significant differences between lease and reference sites were notably rare, suggesting little effect from farm-origin organic loading during this period. Because all three farms were in their first year of culture and fish were small, there were generally low sulfides and little evidence of hypoxia. At the McNutts lease, monthly means of water content, redox, and sulfides all fell within the range of mean reference values. Although sandy, McNutts was not particularly organic-poor. Hartz did show significant differences for farm-reference comparisons in October and November for redox potential and sulfides, but the effects were spatially inconsistent for each successive month. Sandy displayed the greatest range in all variables



of all three sites for both lease and reference values. High sulfides and low redox were frequently observed at multiple locations >100m from the cage edge on the same sampling date, suggesting a much larger zone of effect than both Hartz and McNutts. Heterogeneity was present to some degree throughout the present study and EMP observations, where benthic response to organic loading was highly variable within lease and reference sites and between months. While variability between seasons is expected due to large-scale weather and ocean patterns, heterogeneity in the benthos at the lease scale is not as straightforward. The strong localized response to organic loading frequently observed indicated a source of heterogeneity at a scale smaller than the cage array since organic waste is dispersed during transport to the sediment, not concentrated. Intact or degraded food pellets occasionally observed in sediments are likely sources of small-scale variation since they are hotspots of POM decomposition.

Beyond the present study, EMP observations provided further distinction between sites, although use of historical data requires the caveats below. While substantial changes in benthic conditions between years can be expected, some may be the result of sampling artefacts or longer term changes in aquaculture practices. Water content values below two standard deviations of the mean were not uncommon at Sandy and Hartz. Both sites contained patchy grain size composition, and the location of grab samples can lead to subsequent variation in water content. Aquaculture feed wastage was historically estimated to be much higher at ~20% (Beveridge, 1987) than it is today at 3-8% (Cromey et al. 2002; Stucchi et al. 2005, Chang et al. 2014), and practices such as manual feeding are less efficient than automated feeders. Feed composition in terms of ingredients and lability have also changed over the years of the EMP record. For example, a gradual shift from wet

(~65% dry matter) to dry feeds (~94% dry matter) began at least 25 years ago as advances in distribution, ingredients, price, and storage improved, and have slowly been reduced to only being used at the start of the growth cycle (A. Donkin, personal communication, May 25<sup>th</sup>, 2021). Moreover, the long time series of the EMP data involved multiple sampling personnel, and we cannot assess operator error in the data record. Samples were also collected at various times of year in a strongly seasonal temperate environment. Similarly, beyond feed composition, husbandry occurred over an extended period at the farms in some cases with more than one company and likely differing farming practices. Finally, the details of stocking and fallowing were not available due to confidentiality and our designation of farm culture status was simply binary.

On the basis of the cautions about EMP data discussed above, coarser sediments at McNutts were relatively less sensitive to organic loading, but evidence of organic enrichment was still present. The high levels of sulfides observed in 2011, 2014, and 2018, were paired with increased POM and reduced redox potential, however these relationships were inconsistent between years and when compared to Hartz and Sandy. Redox potential in the EMP data was on average ~150mV higher than at Hartz and Sandy, suggesting that farm-origin POM at McNutts may have had greater access to oxic metabolism in the sediment. These instances of rapid recovery allowed the McNutts farm to were able to continue culture without extended fallow periods like at Hartz and Sandy. However, McNutts also had a more consistent record of farming operations by a single company compared to the two Shelburne Harbour sites.

Though separated by only a few kilometers, Hartz consistently displayed higher levels of POM and water content than Sandy, most likely due to its proximity to the town

of Shelburne and reduced current field of the harbour. In 2008-2009, decreases in POM and sulfides and an increase in redox potential would be expected from an extended following period of 12+ months, however, the opposite occurred at Hartz before fish were reintroduced in 2010. An initial decrease in the POM means from 2007-2008 was followed by the greatest increase in means between adjacent years from 2008-2009. Additionally, the corresponding redox and sulfide values were not aligned with what would be expected with such a high increase in POM of aquaculture origin at Hartz, with an increase in redox and a relatively low increase in sulfides. This suggests that the increase in POM was most likely due to an irregular event that distributed an extended supply of more refractory POM throughout a spatial domain large enough to capture one reference site in 2010 and therefore not likely due to the presence of aquaculture.

However, Hartz appeared to have been less sensitive to culturing practices over the years. Of the observed variables, only lease sulfides and reference redox values from the present study were significantly higher when compared to EMP references. Unlike Sandy, significant differences between present study redox and sulfides for lease and reference values suggested independence. Additionally, Hartz was observed to only display significant increases to sulfides from the farm in November, however this occurred without significant change to POM content. This pattern was different from EMP data, where Hartz was frequently observed to have the lowest sulfides based on changes to POM content.

From 2004-2019, Sandy was more active than Hartz, with nine years of culture compared to six, respectively. During this time, rates of change in sulfide levels compared to increases in POM were far greater at Sandy than Hartz. Additional benthic studies including geochemistry and faunal surveys were conducted at Sandy between 2011-2013

(McGregor Geoscience Ltd., 2012; McGregor Geoscience Ltd., 2013; Milewski, 2014). Sandy was decommissioned as a culture site in 2011 and was neglected in its last years of farming. The rapid increases in sulfides compared to Hartz from 2006-2007 and 2009-2010 could be the result of poor farm management including feed waste and fouled nets. Following decommission, faunal studies indicate a decline in both biodiversity and abundance from 2011-2013. *Capitella capitata*, an indicator species for organic loading (Pearson & Rosenberg, 1978), was the dominant species at some sample stations located under the lease in both 2011 (McGregor Geoscience Ltd., 2012) and 2013 (Milewski, 2014). POM remained high despite decreasing sulfides in 2012. Methanogenesis becomes the dominant pathway for POM mineralisation below a redox potential of -200 mV (Barbera et al., 2019), a value frequently observed between 2007-2012 at Sandy. Lack of faunal recovery and elevated POM suggest continued anoxic sediments in this scenario.

#### *2.4.2 EMP Vs. Present Study*

Differentiating EMP data from the present study is important in determining the natural variability and context of reference values for all variables. At McNutts, lease and reference values of POM and redox potential from the present study were significantly lower than historical EMP reference values, whereas present reference sulfides were significantly higher. The high sulfide and low redox reference values were always observed at the same location, behind the feeding barge. This case provided a clear example of the importance of heterogeneity and spatial scale. The ability to pinpoint an individual source (such as a feeding barge) of greater benthic response is lost when observations are scaled up or summarized to values without spatial dimensions.

In 2019, the cage array for Sandy was moved a few hundred meters north of its prior location, likely changing area of depositional footprint overlap between years. A bay scale mapping study conducted by Bravo (2017) used acoustics and benthic geochemistry to determine bottom type in Shelburne Harbour. Those results indicate that the movement north in 2019 placed the cage array above a mud/sandy-mud sediment type compared to the previous sand/sandy-mud type. This would explain the higher water content observed at the lease during the present study. Lease values from the present study at Sandy were higher in sulfides, and both lease and reference values were lower in redox than EMP reference. Bravo (2017) deployed sediment traps and observed higher levels of ambient POM flux near Sandy compared to Hartz. The ocean outfall from the wastewater treatment facility for Shelburne is located just north of this area. A combination of sewage outfall and aquaculture detritus input to the Sandy site could influence differences in benthic response compared to Hartz. These potential for cumulative effects demonstrates the non-local conditions essential for consideration in EAA.

#### *2.4.3 Geochemical Relationships*

The Hargrave model presents an idealized relationship comprised of an aggregate of historical observations, designed to improve a previous linearized model (Wildish et al., 1999). In the present study, RSE and  $R^2$  values were found to be very similar between the nonlinear exponential and linear models designed for each individual lease when the whole dataset was considered. However, once redox values  $\geq 0\text{mV}$  are removed, each site fit significantly better to both the Hargrave model and the nonlinear exponential model herein. This was expected as the purpose of making the model nonlinear was to address the absence of correlation between sulfide and positive redox values (Whitfield, 1969). Therefore,

though McNutts did produce a better fit to the Hargrave model than Sandy and Hartz, this is most likely due to noise. Differences in positive x-asymptotes for the nonlinear exponential models at Sandy and Hartz offered insight to differences in benthic response at high levels of POM retainment in the sediment. At Sandy, the positive x-asymptotes aligned well with the Hargrave model, approaching infinity near a redox potential of -200mV. However, the model fit around the positive x-asymptotes at Hartz was poor due to the low number of high sulfide values and the lower sulfide response to decreased redox compared to Sandy. These results suggest that lower levels of sulfide are indicative of reduced sediments in Shelburne Harbour than in previous studies.

#### *2.4.4 Acoustics*

At Sandy and Hartz, one of the two designated bottom signatures occurred infrequently, both throughout the domain and at specific sampling locations, preventing adequate data for analysis. In addition, sediment heterogeneity in Shelburne Bay was more substantial than contrasts between farm and reference sediments. Though spatial divisions between signatures appeared to align with either the direction of the prevailing current or proximity to the coastline, a lack of significant differences between geochemical variables along those divisions prevented conclusions being made in that regard. Analysis did produce significant differences between dissolved sulfides for the bottom signatures at Hartz in August, but there was insufficient evidence to suggest this difference was the result of organic loading from the farm. Lower sulfide values are often subject to higher noise and variability than larger values, and mean sulfides at Hartz were  $\sim 100\mu\text{M}$  at both lease and reference sites in August. In the Wildish et al. (2004) study, differences between lease and reference site means of porosity, POM, redox, and sulfides were large compared to the

values in the present study. Therefore, the use of single-beam echo sounding, as opposed to multi-beam, should not be dismissed as a viable method for determining the spatial extent of deposition footprints until assessed under similar benthic conditions to Wildish et al. (2004).

#### *2.4.5 Ecosystem Approach to Aquaculture*

Benthic monitoring and the accompanying managerial responses work towards fulfilling the principles of EAA; that aquaculture should consider all ecosystem functions and services and be designed in a way that does not compound negatively with other sectors (Soto et al., 2007). With respect to benthic response, this is most effectively achieved by constraining farming decisions through an understanding of differences in relationships between sulfide and POM accumulation rates spatially and temporally. Assimilative capacity is the threshold an ecosystem has to integrate foreign matter without achieving a specific response. With respect to aquaculture, assimilative capacity can be defined as the limits of POM integration into the ecosystem while maintaining oxic conditions (Omori et al., 1994). This has previously been estimated in Shelburne as a net accumulation of  $0.62 \text{ gC m}^{-2} \text{ d}^{-1}$  into the sediment over a 1.5 year period before a sulfide concentration of  $1500 \mu\text{M}$  is reached (Bravo & Grant, 2018). However, assimilative capacity alone is insufficient in summarizing benthic response. In ecology, resiliency is the ability of an ecosystem to both resist and recover from impacts of foreign matter integration (Holling, 1973; Holling, 1996), adding an additional dimension to site distinction. Quantifying resiliency can be quite difficult (Standish et al., 2014) and tends to be defined and discussed through qualitative thresholds (Standish et al., 2014; Greenfield et al., 2016; Keeley et al., 2019), but some methods of quantification with respect to aquaculture have occurred

(Kluger et al., 2017). For the present study, qualitative descriptions of assimilative capacity and resiliency are sufficient in distinguishing the three sites. A site like McNutts might be considered to have a high resiliency and low assimilative capacity, where high levels of sulfide were observed on a few occasions when relatively low increases in POM content were found, however the return to oxic conditions was frequently more rapid and sustained than other sites. Hartz would be considered to have both high resiliency and assimilative capacity, as large integrations of POM to the sediment resulted in mean sulfide values that never surpassed  $3000\mu\text{M}$ , and lease and reference values rapidly achieved significant similarity once culturing was stopped in 2012. Sandy would be considered to have both low resiliency and assimilative capacity. Large, sustained increases to sulfides were observed with less organic enrichment than Hartz, and significant differences between lease and reference values continued to be observed for four years after fish were removed in 2011. The benthic response to organic enrichment at each of these sites is linked to larger scale factors than the biological and geochemical composition of the immediate area. Differences in sources of ambient POM flux, historical culturing practices, and proximity to other industrial sectors most likely play a key role in the unique resiliency and assimilative capacity found at each site and should all be considered in tandem moving forward.



## **CHAPTER 3**

### **DIAGENIX: BENTHIC DIAGENESIS MODELLING TO INFORM ENVIRONMENTAL MANAGEMENT STRATEGIES**

#### **3.1 Introduction**

Waste material from ocean-based fish farms includes feces and uneaten food which settles to the benthos. Excess organic input alters sediment communities from oxic to hypoxic to anoxic as benthic metabolism shifts from aerobic to anaerobic usually dominated by sulfate reduction. The consequence of sulfate reduction is release of sulfides which are toxic to aerobes. For this reason, the interstitial concentration of sulfides is used in some regulatory regimes as an indicator of eutrophication caused by aquaculture wastes (AAR, 2018). Despite the importance of sulfide as a regulatory variable, modelling has not been applied in this context.

The response of benthic communities to particulate organic matter (POM) loading is based on its chemical composition, physical characteristics of the sediment, and successional stages of benthic organisms (Pearson & Rosenberg, 1978). Analysis of the relationship these variables share with rates of POM mineralisation and sulfide accumulation allows for distinctions to be made between lease sites. Ideally, the host environment of an aquaculture lease would be one where integration of farm POM into the sediment would infrequently result in a reduced state, and when reduced sediments were observed, recovery was rapid and hysteretic change avoided. Using geochemical measures to determine sediment health can be considered more desirable than macrobenthic abundance and diversity measures, not only because of cost-effectiveness, but also evidence that geochemical measures can be more sensitive at detecting changes in

sediments under fish farms (Hargrave et al., 1997; Wildish et al., 1999). When oxygen is abundant, aerobic respiration is the primary metabolic pathway for POM degradation in the sediment. However, if the presence of POM is high enough, oxygen reserves can become sufficiently depleted and sulfate reduction becomes the primary metabolic pathway (Jørgensen, 1977; Canfield, 1989).

Canadian management methods for aquaculture outline a combination of reactive and proactive strategies for addressing environmental issues. Proactive strategies include the modelling of POM deposition for initial site assessment and site expansion, with results used to determine monitoring intensity and sampling locations within and surrounding the lease (NSDFA, 2019a; AAR, 2018). DEPOMOD is the most widely used software for depositional modelling in Canada. Developed in Scotland, DEPOMOD estimates the benthic response to predicted POM deposition using the Infaunal Trophic Index and total abundance (Cromeley et al., 2002), and has been utilized by numerous private and government stakeholders in environments across Canada (Weise et al., 2009; Chang et al., 2014) and other countries (Cromeley et al., 2012; Keeley et al., 2013; Adams et al., 2020). DEPOMOD relies on single point current velocity for diffusion/advection rather than detailed circulation. While DEPOMOD has provided beneficial information for regulation (Hargrave, 2010; DFO, 2012; Chang et al., 2014), the absence of a diagenetic component oversimplifies the relationship between POM deposition and benthic health. Prior models have attempted to simulate or compare benthic response to aquaculture loading with varying levels of success (Brigolin et al., 2009; Chang et al., 2014; Bravo & Grant, 2018), but a model optimized for sulfide response and scalability is not readily available. Modelling applied within the framework of current regulatory methods that considers both

farm deposition and the resulting changes to diagenesis would reduce long-term environmental impacts by providing stakeholders with information to influence management decisions such as interactions between lease sites and the benthos, best stocking and feeding practices, and effects of hydrodynamic and weather activity.

To predict these sulfide complexes, this research was centered around the development of a reaction-transport numerical model of early diagenesis (DIAGENIX) to simulate vertical redox zonation, zonation influence on organic carbon ( $C_{org}$ ) degradation, and dissolved sulfides. In its final form, DIAGENIX will be utilized to model grid cells independently throughout bay-scale ecosystems, with variable deposition inputs received from coupled deposition and hydrodynamic models not considered in the present study. Model outputs will be assembled to produce contour maps of benthic health categories, consisting of grid cells of adjustable size, allowing for spatial and temporal patterns to be visualized.

Sediment transport parameters, such as advection, diffusion, bioirrigation, and bioturbation, are not only depth-dependent but influenced by sediment toxicity of sulfides. Two types of sulfate reduction metabolites were of primary interest in the present study: sulfides dissolved in porewater that are considered toxic to benthic invertebrate ( $H_2S$ ,  $HS^-$ , and  $S^{2-}$ ) and metal sulfide complexes that are not considered toxic in their current form ( $FeS$  and  $FeS_2$ ). Toxicity of dissolved sulfides varies depending on species of benthic invertebrates (Wang & Chapman, 1999), but category thresholds for benthic health quality have been determined provincially for Nova Scotia (Hargrave et al., 2008) based upon prior organic enrichment studies (Wildish et al., 2001; Cranford et al., 2006). Dissolved sulfides  $>1500\mu M$  are considered to be hypoxic (Hargrave et al., 2008; NSDFA, 2019b), and

therefore beginning to adversely effect the benthic community. Regulatory measures in Nova Scotia are heavily influenced by sulfide accumulation, yet this focus on sulfides is notably absent for site modelling.

In the present study, DIAGENIX was calibrated to be used in conjunction with observations from the environmental monitoring program (EMP) established and regulated by the Nova Scotia Department of Fisheries & Aquaculture (NSDFA). Model outputs were validated through comparison of EMP observations taken from two different aquaculture sites in Shelburne Harbour of Nova Scotia between 2004-2019. Salmon and trout have been farmed in the area at a variety of intervals over the past 30+ years, providing a broad spectrum of data to be used for model parameter adjustment and validation, however the most comprehensive data was found to be from 2004 onwards. A prior study collected benthic geochemistry and sediment trap observations throughout Shelburne Harbour in 2014 (Bravo, 2017), providing one of the most comprehensive mappings of a large portion of the sample area to date. All previous data were used to determine appropriate ambient conditions (no POM input from farm), steady state variables, and transient state variables for hindcasting and forecasting. Objectives were as follows:

- Calibrate model to establish appropriate initial conditions in the vertical dimension for hypoxic/anoxic/sulfidic sediment profiles for study sites
- Use groundtruthing sample sites from provincial monitoring data to establish an ambient/production/fallowing timeline for each site
- Validate model through comparison of simulations to study sites while limiting adjustments to parameters and state variables to those found in Shelburne Harbour

- Determine if model accuracy and sensitivity are maintained throughout an acceptable range of values for parameters likely to differ between sites

## 3.2 Methods

### 3.2.1 *DIAGENIX* structure

The DIAGENIX model development framework was based on a method-of-lines technique frequently utilized in marine diagenesis models (Boudreau, 1996), allowing for both steady-state and transient scenarios, multiple redox states, and manipulation of depth-dependent characteristics such as bioturbation, bioirrigation, and porosity. Determination of elemental cycles to include in DIAGENIX was based on an idealized set of equations around the molecular exchange and burial of sulfur (Table 3.1).

Due to the emphasis on sulfate as a regulatory variable, the sedimentary sulfur cycle was the primary focus of DIAGENIX. In addition, field samples for dissolved sulfides under Canadian protocols integrate the top 2cm in syringe cores, and model output was presented with identical integration. Nitrate and manganese reduction were omitted from the model under the assumption of inconsequential influence on the sulfur cycle and were reserved to earlier stages of POM loading (Bravo & Grant, 2018). However,  $\text{Fe}(\text{OH})_3$  and  $\text{Fe}^{2+}$  were retained for model development as the presence of iron minerals in marine sediments heavily influence sulfate reduction rates (Thamdrup et al., 1994). The methanic zone, below the sulfidic zone, was omitted under the assumptions that whether the terminal process is one involving iron, sulfate, or methane is of no consequence to initial hydrolytic activity and overall rates of POM degradation (Beulig et al., 2018), and that the influence of methane on S, O, and Fe cycles is limited.

Reactive POM pools in the model were degraded through oxic respiration, sulfate reduction, and iron reduction. For redox reactions, oxidant limitation was represented through Monod-type hyperbolic functions and inhibition terms through reciprocal hyperbolic functions, with reduced metabolites either re-oxidized or precipitated. The simplified diagenetic model reaction network was limited to chemical species involved in the elemental cycles of C, O, Fe, and S (Figure 3.1).

Table 3.1: Idealized primary and secondary redox reactions utilized in the model. TS = HS<sup>-</sup> + H<sub>2</sub>S.

<b>Redox reaction</b>	<b>Equation</b>	<b>Eq.</b>
Aerobic respiration	OM + 1.3O <sub>2</sub> → CO <sub>2</sub> + H <sub>2</sub> O	(R1)
Fe <sup>III</sup> reduction	OM + 4Fe(OH) <sub>3</sub> + 7CO <sub>2</sub> → 4Fe <sup>2+</sup> (aq) + 8HCO <sub>3</sub> <sup>-</sup> + 3H <sub>2</sub> O	(R2)
Sulfate reduction	OM + 0.5SO <sub>4</sub> <sup>2-</sup> (aq) → 0.5H <sub>2</sub> S + 2HCO <sub>3</sub> <sup>-</sup>	(R3)
Fe <sup>II</sup> oxidation by O <sub>2</sub>	Fe <sup>2+</sup> (aq) + 0.25O <sub>2</sub> + 2HCO <sub>3</sub> <sup>-</sup> + 0.5H <sub>2</sub> O → Fe(OH) <sub>3</sub> + 2CO <sub>2</sub>	(R4)
Sulfide oxidation by O <sub>2</sub>	TS + 2O <sub>2</sub> + 2HCO <sub>3</sub> <sup>-</sup> → H <sub>2</sub> O + SO <sub>4</sub> <sup>2-</sup> + 2CO <sub>2</sub>	(R5)
Sulfide oxidation by Fe <sup>III</sup>	TS + 2Fe(OH) <sub>3</sub> + 5H <sup>+</sup> → 2Fe <sup>2+</sup> (aq) + SO <sub>4</sub> <sup>2-</sup> (aq) + 6H <sub>2</sub> O	(R6)
FeS precipitation	Fe(aq) + TS → FeS(s) + H <sup>+</sup>	(R7)
FeS oxidation	FeS(s) + 2O <sub>2</sub> → Fe <sup>2+</sup> (aq) + SO <sub>4</sub> <sup>2-</sup> (aq)	(R8)
Pyrite precipitation	FeS(s) + TS → FeS <sub>2</sub> (s) + H <sup>+</sup>	(R9)

The model was based on a series of non-linear partial differential equations (PDEs) of the form:

$$\frac{\partial C}{\partial t} = T + R \quad (\text{Eq. 3.1})$$

where C is concentration (mass/volume), t is time, T is transport (mass/volume/time), and R is reaction (mass/volume/time). The transport component is further broken down into advection and diffusion patterns throughout the sediment column, with respect to time:

$$\varphi_s \frac{\partial S_i}{\partial t} = -\varphi_s \frac{\partial}{\partial z} \left( w_{\text{sed}} S_i - K_v D_b \frac{\partial S_i}{\partial z} \right) + \sum R(S_i, C_i) \quad (\text{Eq. 3.2})$$

$$\varphi \frac{\partial C_i}{\partial t} = -\varphi \frac{\partial}{\partial z} \left( w_{\text{pw}} C_i + D \frac{\partial C_i}{\partial z} \right) + K_v v(C_{i,0} - C_i) + \sum R(S_i, C_i) \quad (\text{Eq. 3.3})$$

where  $S_i$  and  $C_i$  are the concentration of solid and dissolved species,  $z$  is the depth below the sediment water interface (SWI),  $\varphi$  is sediment porosity and  $\varphi_s$  the solid fraction,  $D_b$  is bioturbation and  $D$  is the total molecular diffusion plus bioturbation,  $w_{\text{sed}}$  is solid burial rate and  $w_{\text{pw}}$  is porewater burial rate, and  $\Sigma R$  represents the net rate of concentration change due to chemical reaction sources and sinks (Table 3.2). The vertical 1D spatial component of the model had a sediment depth of 30cm and was divided

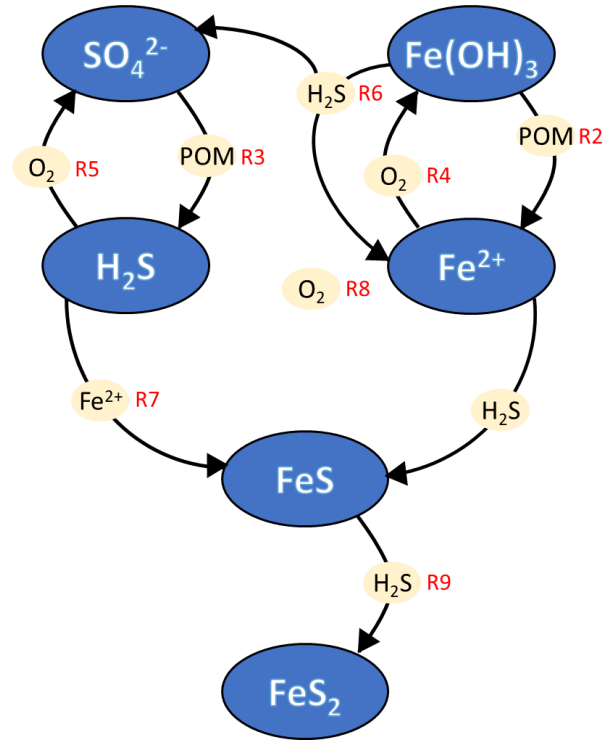


Figure 3.1: Reaction network of chemical species interactions under consideration in diagenetic model.

into 60 layers, with a resolution gradient having a finer discretization originating at the SWI because the processes that occur near the sediment surface are more numerous and occur at greater rates than at depth (Fossing et al., 2004), and because of the importance of the upper 2cm of sediment for provincial monitoring. These transport components were not homogenous throughout the sediment column; as depth below the SWI increases,

nonlinear changes occur to fundamental parameters such as bioturbation, bioirrigation, and porosity.

Table 3.2: Summary of model equations. OM: Organic matter;  $\phi_s$ : Sediment solid fraction; R: Reaction;  $i = 1, 2$ . See Table 3.3 for reaction terms.

<b>Reaction</b>	<b>Eq.</b>	
$\Sigma R(OM_i)$	$= - (R1 + R2 + R3)$	<i>S1</i>
$\Sigma R(O_2)$	$= - (\phi_s/\phi) * R1 - R4 - R5$	<i>S2</i>
$\Sigma R(FeOH_3)$	$= + (\phi/\phi_s) * R5 - R3 - R6$	<i>S3</i>
$\Sigma R(SO_4)$	$= - (\phi_s/\phi) * R2 + R4 + R6$	<i>S4</i>
$\Sigma R(TS)$	$= + (\phi_s/\phi) * (R2 - R4 - R6 - R7)$	<i>S5</i>
$\Sigma R(Fe)$	$= + (\phi_s/\phi) * (R3 - R5 - R7)$	<i>S6</i>
$\Sigma R(FeS)$	$= + R7 - R8$	<i>S7</i>
$\Sigma R(FeS_2)$	$= + R8$	<i>S8</i>

Table 3.3: Rate equations used in model equations. See Table 3.4 for parameter terms.

<b>Rate equation</b>	<b>Eq.</b>
$MinRate_i * [OM_i] * ([O_2] / ([O_2] + k_{O2lim}))$	<i>R1</i>
$MinRate_i * [OM_i] * ([Fe(OH)_3] / ([Fe(OH)_3] + k_{FeOH3lim})) * (k_{inO2} / (k_{inO2} + [O_2]))$	<i>R2</i>
$MinRate_i * [OM_i] * ([SO_4] / ([SO_4] + k_{SO4lim})) * (k_{inO2} / (k_{inO2} + [O_2])) * (k_{inFeOH} / (k_{inFeOH} + [O_2]))$	<i>R3</i>
$k_{SoxO2} * [TS] * [O_2]$	<i>R4</i>
$k_{FeoxO2} * [Fe^{2+}] * [O_2]$	<i>R5</i>
$k_{SoxFeOH} * [TS] * [FeOH_3]$	<i>R6</i>
$[Fe^{2+}] * [TS] < K_{FeS_{sp}} \rightarrow 0$	<i>R7</i>
$[Fe^{2+}] * [TS] > K_{FeS_{sp}} \rightarrow k_{FeS} * ([Fe^{2+}] * [TS] - K_{FeS_{sp}})$	
$k_{FeS2} * [FeS]$	<i>R8</i>

Other than advective and diffusive transport processes, chemical species are transported through sediment by the depth-diminishing biologically mediated processes of bioturbation and bioirrigation (Jørgensen et al., 2019). In DIAGENIX, bioirrigation is defined as an exchange of solute chemical species between the sediment and overlying water, based on differences in solute concentrations above and below the SWI, as well as a velocity coefficient (Hammond & Fuller, 1979):

$$Bioirrigation = K_v v (C_{i,0} - C_i) \quad (\text{Eq. 3.4})$$



where  $C_{i,0}$  is concentration of solute at the SWI,  $C_i$  is concentration of solute within the sediment, and  $v$  is exchange velocity of solutes due to bioirrigation.  $K_v$ , was added to represent the toxic effects of dissolved sulfide in the sediment porewater:

$$\left. \begin{aligned} K_{\text{voxic}} &= 1 && \text{for } [\text{H}_2\text{S}] < 1500\mu\text{M} \\ K_{\text{vhyoxic}} &= (1 - ([\text{H}_2\text{S}]/10,000)) && \text{for } 1500\mu\text{M} < [\text{H}_2\text{S}] < 10,000\mu\text{M} \\ K_{\text{vanoxic}} &= 0 && \text{for } [\text{H}_2\text{S}] > 10,000\mu\text{M} \end{aligned} \right\} \text{(Eq. 3.5)}$$

where the total sulfides in the sediment are compared to the  $10,000\mu\text{M}$  reference term, considered to be lethal to the organisms most responsible for bioirrigation (Bravo & Grant, 2018). A generalized bioturbation coefficient is necessary to account for all remaining biologically mediated fluctuations in solid or solute concentrations with time (Boudreau, 1986; Boudreau, 1997). Intrapphase mixing was chosen for DIAGENIX because it accounts for irrigation of porewaters (Boudreau, 1997):

$$\text{Flux} = -\phi D_B \frac{\partial C}{\partial x} \quad \text{(Eq. 3.6)}$$

Porosity and  $D_b$  values were assigned similar vertical structure, with a uniform value throughout the biologically active layer, dropping off exponentially to zero from 5-10cm to reflect previously observed biologically active layers in Shelburne sediments (Simone & Grant, 2017). The value of sedimentation velocity  $\omega$  was dependent on flux of POM to the sediment (Meysman et al., 2005) with an assumption of steady-state compaction for porosity represented through:

$$\omega = F / (\rho (1 - \phi)) \quad \text{(Eq. 3.7)}$$

where  $F$  is flux of POM from the farm and  $\rho$  is POM density.

### 3.2.2 Parameterization

Constant parameters, such as reaction velocities, limiting coefficients, and diffusion coefficients, were selected based on the literature, while solute boundary conditions were calculated from temperature and salinity values of overlying seawater (Table 3.4).  $C_{org}$  content of farm-origin fluxes was based on salmon food, feces, and ambient deposition and was set to 40% for each pool of POM. Deposition fluxes to the sediment used in DIAGENIX were divided into three pools, differentiated by rapid (labile), moderate (semi-labile), and slow (refractory) mineralisation rates of  $C_{org}$ , similar to the G-model (Westrich & Berner, 1984). Mineralisation rates of  $C_{org}$  were constrained to reflect geochemical relationships observed in Shelburne Harbour. This was accomplished through an establishment of upper and lower limits for the ratio between sulfide and POM concentrations based on observations from the EMP data. Mineralisation rates of the individual pools were then adjusted to allow for the potential range of values between these upper and lower limits to be achieved within the simulation time frame. Rates for each POM pool were assumed to be consistent throughout the modelled sediment column domain. Ambient state of the model was estimated through running simulations to steady-state with relatively low deposition fluxes similar to those found in Bravo (2017) and were compared to EMP observations outside of fish farm influence. Manual adjustments of porosity and content of semi-labile and refractory  $C_{org}$  fluxes were chosen to reflect means of porosity, POM, and dissolved sulfide of respective reference sites.

Table 3.4: Model parameters and boundary conditions used in DIAGENIX.

Parameter	Description	Value	Units	Reference
$k_{\text{SoxO}_2}$	Sulfide oxidation rate with $\text{O}_2$	164.4	$\text{cm}^3\mu\text{mol}^{-1}\text{d}^{-1}$	Boudreau (1996)
$k_{\text{SoxFeOH}}$	Sulfide oxidation rate with $\text{Fe}(\text{OH})_3$	0.0356	$\text{cm}^3\mu\text{mol}^{-1}\text{d}^{-1}$	Brigolin et al. (2009)
$k_{\text{FeoxO}_2}$	Rate constant for $\text{Fe}^{2+}$ oxidation with $\text{O}_2$	109.6	$\text{cm}^3\mu\text{mol}^{-1}\text{d}^{-1}$	Bravo (2017)
$k_{\text{FeS}_2}$	Rate constant for $\text{FeS}_2$ formation from $\text{FeS}$	$2.73\text{e}^{-6}$	$\text{d}^{-1}$	Boudreau et al. (1998)
$k_{\text{FeS}}$	Rate constant for $\text{FeS}$ precipitation from $\text{Fe}^{2+}$	0.821	$\text{cm}^3\mu\text{mol}^{-1}\text{d}^{-1}$	Boudreau et al. (1998)
$D_{\text{H}_2\text{S}}$	Diffusion coefficient for $\text{H}_2\text{S}$ at $14^\circ\text{C}$	0.78	$\text{cm}^2\text{d}^{-1}$	Fossing et al. (2004)
$D_{\text{Fe}}$	Diffusion coefficient for $\text{Fe}^{2+}$ at $14^\circ\text{C}$	0.32	$\text{cm}^2\text{d}^{-1}$	Fossing et al. (2004)
$D_{\text{O}_2}$	Diffusion coefficient for $\text{O}_2$ at $14^\circ\text{C}$	1.04	$\text{cm}^2\text{d}^{-1}$	Fossing et al. (2004)
$D_{\text{SO}_4}$	Diffusion coefficient for $\text{SO}_4$ at $14^\circ\text{C}$	0.48	$\text{cm}^2\text{d}^{-1}$	Fossing et al. (2004)
$k_{\text{O}_2\text{lim}}$	HSC for $\text{O}_2$ limitation in OM	0.004	$\mu\text{mol cm}^{-3}$	Pastor et al. (2011)
$k_{\text{SO}_4\text{lim}}$	HSC for $\text{SO}_4$ limitation in SR	1.6	$\mu\text{mol cm}^{-3}$	Shafei (2012)
$k_{\text{FeOH}_3\text{lim}}$	HSC for $\text{Fe}(\text{OH})_3$ limitation in SR	200	$\mu\text{mol cm}^{-3}$	Specific for this study
$k_{\text{inO}_2}$	$\text{O}_2$ inhibition coefficient	0.01	$\mu\text{mol cm}^{-3}$	Soetaert et al. (1996b)
$k_{\text{inFeOH}}$	$\text{Fe}(\text{OH})_3$ inhibition coefficient	0.01	$\mu\text{mol cm}^{-3}$	Bravo (2017)
$K_{\text{FeS}_{\text{sp}}}$	Solubility product constant of $\text{FeS}$	0.0583	$(\mu\text{mol cm}^{-3})^{-2}$	Boudreau (1996)
$\text{MinRate}_1$	Maximum decay rate for labile OM	0.1	$\text{d}^{-1}$	Specific for this study
$\text{MinRate}_2$	Maximum decay rate for semi-labile OM	0.01	$\text{d}^{-1}$	Specific for this study
$\text{MinRate}_3$	Maximum decay rate for refractory OM	$2.73\text{e}^{-6}$	$\text{d}^{-1}$	Specific for this study
$\varphi_\infty, \varphi_0$	Porosity [upstream,downstream]	0.60,0.75	Unitless	Specific for this study
$\text{O}_2\text{BW}$	Oxygen bottom water	0.265	$\mu\text{mol cm}^{-3}$	Specific for this study
$\text{SO}_4\text{BW}$	Sulfate bottom water	25	$\mu\text{mol cm}^{-3}$	Specific for this study
Irrigdepth	Irrigation depth	7	cm	Simone & Grant (2017)
$\text{H}_2\text{S}_{\text{MAX}}$	Toxic concentration for macrofauna	10	$\mu\text{mol cm}^{-3}$	Fossing et al. (2004)
$v$	Irrigation coefficient	2.13	$\text{cm d}^{-1}$	Morse & Eldridge (2007)
$D_b$	Bioturbation coefficient at SWI	$1.37\text{e}^{-2}$	$\text{cm d}^{-1}$	Soetaert (1996a)

### 3.2.3 Initial Conditions

Initial conditions were based on observations from similar coastal sediment environments not subject to forcing from aquaculture sites, as well as historical site data. Previous samples from Shelburne Harbour during early fish farm development indicated that sediments near cages contained 1.27-2.43% iron and 5.2-10.07% POM (Loring et al., 1996), while EMP observations provided porosity, dissolved sulfides, and POM content from 2004-2019. However, the historical observations only reported values as integrated averages of the upper sediments, failing to provide sufficient data to estimate entire vertical profiles of all species included in DIAGENIX. Therefore, any remaining gaps in vertical profiles of other state variable concentrations were filled from the literature (Hargrave, 1994; Soetaert et al., 1996a; Boudreau, 1996; Wang & Van Cappellen, 1996; Fossing et al., 2004; Meysman et al., 2003; Brigolin et al., 2009) and set to reflect a state of diagenesis upon which  $\text{MnO}_2$  and  $\text{NO}_3^-$  depletion had been reached. These data were then combined with steady-state estimates of 1D profiles for each species using a Newton-Raphson method via the *Steady.ID* function from the *rootSolve* package in the R programming language (Soetaert, 2009; Soetaert & Herman, 2009). The resulting initial states were then run through the model with no additional changes for a period of 1000 days to check for any deviations from *Steady.ID* estimated equilibrium output. These outputs established an ambient state for all simulations similar to validation sites where porosity = 0.75, dissolved sulfides = 200 $\mu\text{M}$ , and POM = 15%.

### 3.2.4 Validation

The performance of DIAGENIX was assessed through groundtruthing by publicly available benthic EMP data from field samples collected between 2004 – 2019, at two sites

within Shelburne Harbour, Nova Scotia (Sandy and Hartz). The sites contained mud to sandy mud and were relatively protected in the inner harbour at depths of ~13m. Due to proximity and similarity in depth, bottom type, and historical culturing practices between these sites, a single set of simulations were intended to represent both farm locations for the purpose of groundtruthing. From 2004-2019, most cultured fish were Atlantic Salmon, historically stocked in late spring or early summer. After stocking, salmon are typically present at the site for an 18 month grow-out period, followed by 4-6 months of fallowing in the winter. Data relating to fish biomass and culture status were available as only presence or absence of fish for each year. Benthic EMP sampling was relegated to occur annually between July and October each year (NSDFA, 2019b), meaning that monitoring occurred either 1-6 or 13-18 months after stocking. Three time points in culture status were designated: ambient state, near-peak biomass (production), and fallowed. An aggregate of all reference observations was used to compare the model to ambient state before deposition characteristics of each farm were applied to the model. The production period was simulated with a median deposition flux of  $5\text{gC m}^{-2} \text{d}^{-1}$  for 15 months to reflect a possible real-world scenario where stocking occurred in May and observations were made late the following summer, a point during the culturing cycle where the farmed fish would be at near-peak biomass before harvesting, producing some of the highest levels of POM deposition. Simulations of fallowing were run for 6 months in the absence of farm deposition while ambient depositions were maintained. The depositional fluxes labels applied to fallow simulations refer to the waste inputs that occurred in the previous production period. Groundtruthing of fallowing was determined by aggregating lease observations taken in years when fish were absent during sampling, whereas

groundtruthing of production was determined by aggregating years when fish were present. Since EMP measurements were not made at each lease sample location immediately following harvest or fallowing, timelines for simulation and observation comparison were not exact.

### *3.2.5 Simulations*

In addition to validating the model through comparisons to EMP observations, a series of hypothetical scenarios were simulated, where changes to labile mineralisation rate, organic pool composition, and biological transport demonstrated potential upper and lower boundaries in response of sulfide and POM content to organic loading. Simulations were conducted in three categories with all simulation sets including a farm flux of 1, 5, and 10 gC m<sup>-2</sup> d<sup>-1</sup>, reflecting thresholds within Canadian regulations. Simulation results were summarized as values of sulfide and POM integrated over the 0-2cm sediment horizon, corresponding to Canadian regulatory variables and allowing comparison to groundtruthing results. In each case, initial conditions were the same and present results at ambient state, following a 15 month production cycle, and following a 6 month fallow period. Simulation were as follows:

- (a) Variations in organic matter pool ratio of labile and semi-labile POM, with the pool of refractory POM remaining at 10% total farm flux. The ratios of labile:semi-labile:refractory were set at 9:9:2, 14:4:2, and 4:14:2.
- (b) Variations in the mineralisation rate of labile POM (0.04, 0.1, and 1 d<sup>-1</sup>)
- (c) Changes to biological transport (1)  $D_b$  is deleted such that solutes are transported by diffusion and irrigation only; (2) Removal of sulfide toxicity;

$D_b$  and irrigation are not weighted by sulfide concentration; (3) Bioirrigation is removed and there is no multiplier for  $D_b$  due to fauna

### 3.2.6 Sensitivity

Sensitivity analysis of parameters for periods of farm production and fallowing was completed using the method outlined in Jørgensen & Bendoriccio (2001):

$$IS\% = \frac{100}{p} * \frac{1}{n} \sum_{i=1}^n \frac{X_i - X_i^{ref}}{X_i^{ref}} \quad (\text{Eq. 3.8})$$

Where IS% is the normalized standard deviation index (percentage of variation in response variable),  $p$  is percentage of variation in the parameter being tested, and  $x_i$  is the tested parameter value to be compared to the reference value,  $x_i^{ref}$ . Variable sensitivity was determined for changes in all three mineralisation pathways, total dissolved sulfides, sulfate concentration, and TOC concentration.

## 3.3 Results

### 3.3.1 Initial state

Simulations in the absence of aquaculture input to sediments produced equilibrium solute profiles reflective of sediment zonation present in an oxic state approaching a suboxic state. Estimation of chemical species profiles using the Newton-Raphson method was able to maintain a consistent steady-state after stability testing for a 1000 day period. The mean sulfide and POM content in the surface of ambient sediments in Shelburne Bay was relatively higher than calibration data used for other coastal diagenetic models, resulting in an initial state where suboxic metabolism had begun to occur at low rates.

Oxygen concentrations dropped sharply within the upper millimeters of the sediment, while differences in mineralisation rate for semi-labile and refractory POM pools resulted in two peaks in the dissolved sulfides profile, with corresponding reductions in sulfate (Figure 3.2). Both  $\text{Fe}^{2+}$  and  $\text{Fe}(\text{OH})_3$  were low but still present in the surface sediments, dropping rapidly to zero within 5cm. Additionally, slight deviations from the otherwise smooth transition patterns occurred in iron species within the first few centimeters below the biologically active layer due to changes in solid and solute transport dynamics.

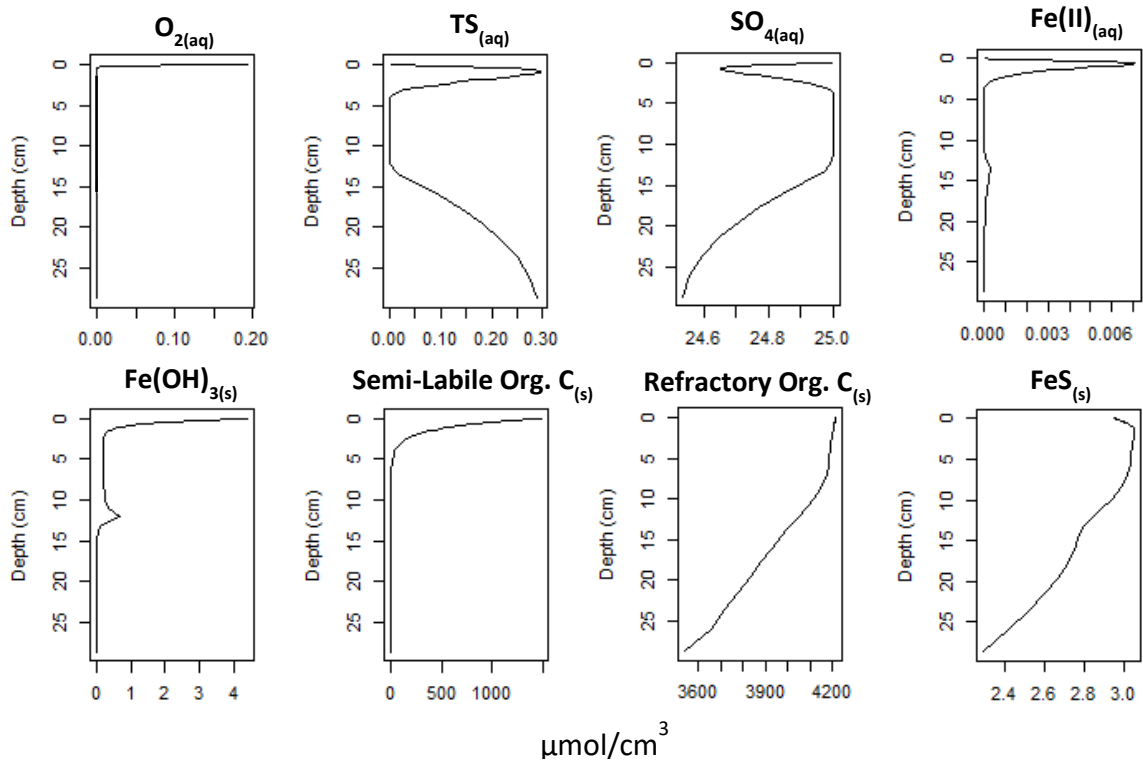


Figure 3.2: Initial state vertical profiles of chemical species involved in diagenetic model. TS = total dissolved sulfides ( $\text{HS}^-$ ,  $\text{H}_2\text{S}$ ,  $\text{S}^{2-}$ ). Units ( $\mu\text{mol}/\text{cm}^3$ ) reflect the concentration of each species with respect to the volume of phase in which they exist.

### 3.3.2 Organic Matter Pool Ratio

Simulations sets varying the proportion of labile and semi-labile organic matter had minimal effect on dissolved sulfide outputs for a given particulate flux level during fish



production (Figure 3.3). In contrast, farm inputs had a major influence on sulfide level. Results from  $1\text{gC m}^{-2}\text{ d}^{-1}$  for all ratio groups produced values of  $600\text{--}700\mu\text{M}$  during fish production and  $200\text{--}300\mu\text{M}$  during fallowing. At  $5\text{gC m}^{-2}\text{ d}^{-1}$ , all ratio groups ended up in hypoxic classification during production at  $3000\text{--}3400\mu\text{M}$ . During fallowing, all ratio groups were above ambient state, with both 9:9:2 and 14:4:2 at  $250\mu\text{M}$ , and 4:14:2 at

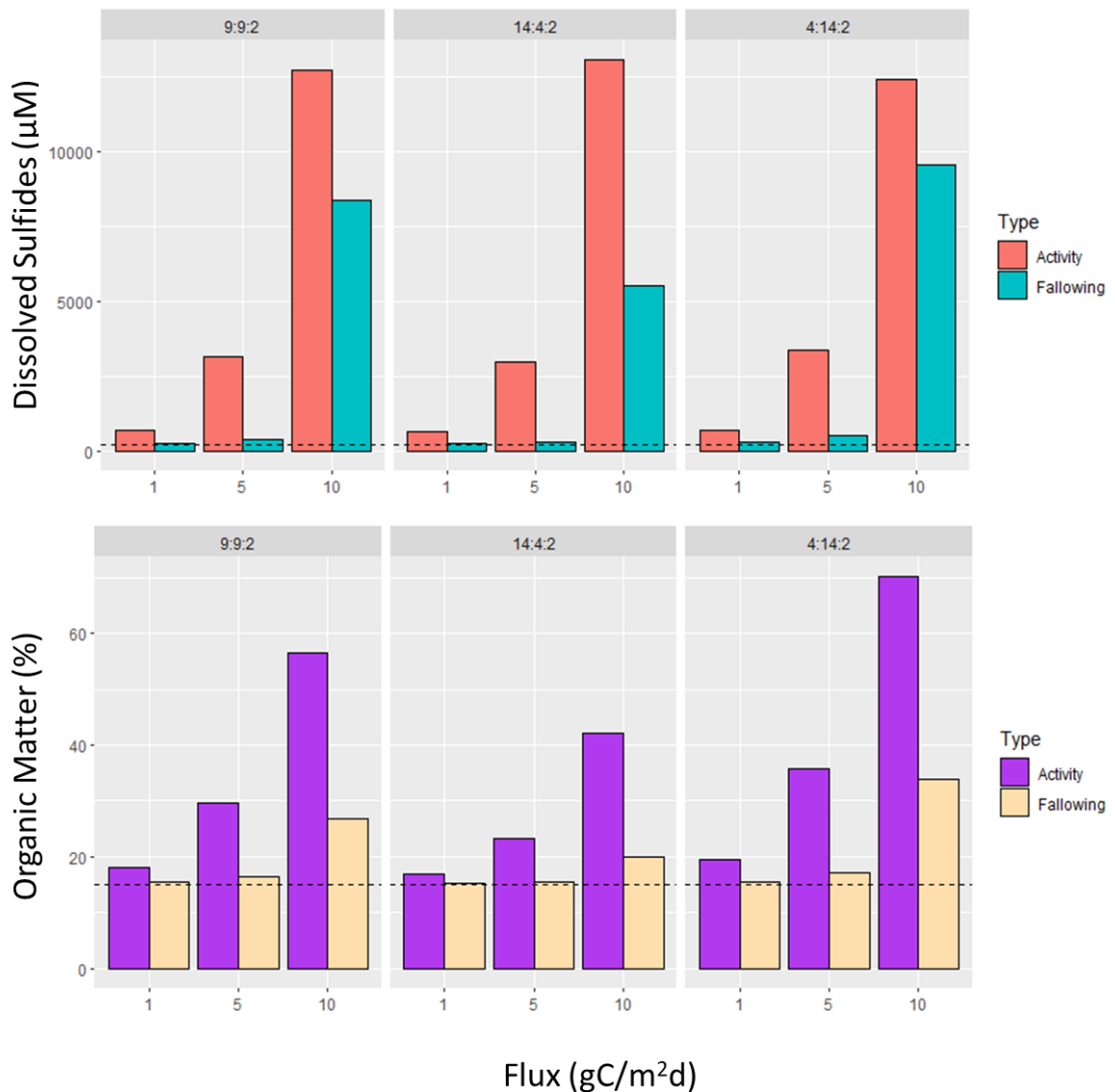


Figure 3.3: Dissolved sulfides and POM content for simulations run with **differing organic matter pool ratios**. ‘Activity’ simulations run for 15 months, and ‘Fallowing’ simulations run for 6 months, with initial Fallowing profiles taken from final Activity simulation output. Horizontal dashed line = initial state.

500 $\mu$ M. While all ratio groups at 10gC m<sup>-2</sup> d<sup>-1</sup> during production were similar (12400-13050 $\mu$ M), sulfides in fallowing were higher in the 14:4:2 pool proportions (7550 $\mu$ M) followed by 9:9:2 (4350 $\mu$ M) and 4:14:2 (2850 $\mu$ M).

Although POM outputs showed similar patterns to dissolved sulfides, there were notable differences. During farming and fallowing at inputs of 1gC m<sup>-2</sup> d<sup>-1</sup>, POM for all ratio categories was similar between 16.9-19.5%, and 15.2-15.6% respectively. Greater differences were observed during production for 5gC m<sup>-2</sup> d<sup>-1</sup>, with 9:9:2 at 29.5%, 14:4:2 at 23.4%, and 4:14:2 at 35.7%. During fallowing, results for both 1 and 5gC m<sup>-2</sup> d<sup>-1</sup> remained within a relatively small range for all ratios (15.2-17.2%). At 10gC m<sup>-2</sup> d<sup>-1</sup>, the differences between the groups during production were more pronounced, with almost doubled POM in the case with smallest relative labile fraction compared to even distribution of labile and semi-labile fractions. Upon fallowing, the 9:9:2 scenario was similar in POM to at all deposition levels but 14:4:2 and 4:14:2 were elevated at an input of 10 gC m<sup>-2</sup> d<sup>-1</sup>.

### *3.3.3 Mineralisation Rates*

Variations in mineralization rate had a major effect on predicted sulfides, especially at higher deposition rates (Figure 3.4A). During production, sulfides from a 1gC m<sup>-2</sup> d<sup>-1</sup> input produced a range of 500-700 $\mu$ M across all mineralisation groups, while 5gC m<sup>-2</sup> d<sup>-1</sup> produced a range of 1600-3650 $\mu$ M. For both 1 and 5gC m<sup>-2</sup> d<sup>-1</sup>, fallowing caused all mineralisation groups to within come 100 $\mu$ M of the ambient state concentration. At 10gC m<sup>-2</sup> d<sup>-1</sup>, the fastest mineralisation rate was differentiated by developing a final concentration nearly 10,000 $\mu$ M below that of the two lower mineralisation rates (3400 $\mu$ M). Both 0.1 and 0.04 d<sup>-1</sup> mineralisation rates appeared to be approaching a plateau at ~13,000 $\mu$ M sulfide

during production. Although higher mineralization might be expected to yield higher sulfides, near surface diffusion inhibits their accumulation. In contrast, particulate accumulation associated with greater deposition allows buildup of sulfides arising from metabolism of buried POM. This is observed in simulation of POM, with much greater values at higher deposition rates during production (Figure 3.4B). During following for the

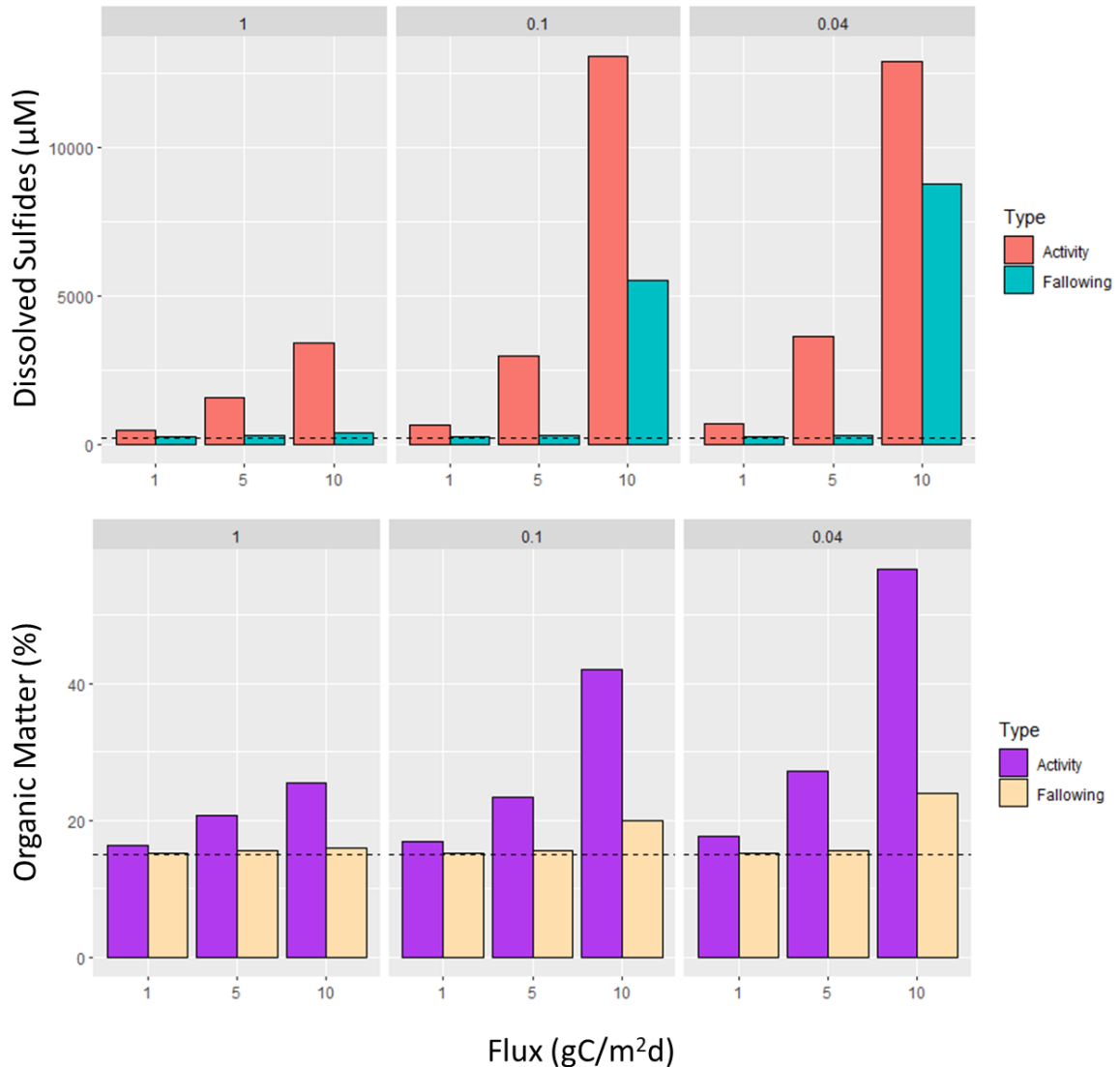


Figure 3.4: Dissolved sulfides and organic matter content for simulations run with **differing labile decay rates (d<sup>-1</sup>)**. ‘Activity’ simulations run for 15 months, and ‘Following’ simulations run for 6 months, with initial Following profiles taken from final Activity simulation output. Horizontal dashed line = initial state.

10gC m<sup>-2</sup> d<sup>-1</sup> scenarios, the most rapid mineralisation rate began to approach ambient levels (350µM), while 0.1 d<sup>-1</sup> moved from anoxic to hypoxic at (5500µM), and 0.04 d<sup>-1</sup> remained anoxic (8800µM).

Simulated POM concentration during production correlates with outputs from modelled sulfides, with increased accumulation following increases in depositional flux, and an inverse relationship between deposition and mineralisation rate. During production at 1gC m<sup>-2</sup> d<sup>-1</sup>, POM responded weakly to changes in mineralization rate with a slightly stronger response at at 5gC m<sup>-2</sup> d<sup>-1</sup>. At deposition rates of 10gC m<sup>-2</sup> d<sup>-1</sup>, mineralization rate had a major impact on POM, almost doubling organic content from 1 d<sup>-1</sup> compared to 0.04 d<sup>-1</sup>. This differential was greater for POM than for sulfides simply because POM accumulates in surficial sediments compared to dissolved sulfides that are lost by diffusion and oxidation. In contrast, during fallowing, variations in POM were not greatly affected by mineralization rate, likely because of the increase in mineralisation rate at higher POM values; especially near the surface due to overlying water renewal.

#### *3.3.4 Transport Parameters*

The removal of the D<sub>b</sub> parameter from the model caused dissolved sulfide levels during production to be lower than all other scenarios (Figure 3.5). Absence of D<sub>b</sub> also produced very low sulfide levels during the fallowing period (50-250µM). Elimination of the H<sub>2</sub>S toxicity parameter left biologically mediated transport unmitigated and had a somewhat larger affect on sulfide than deletion of D<sub>b</sub>. These outcomes were the result of the significantly reduced burial of POM upon removal of D<sub>b</sub>. This caused the majority of mineralisation to occur near the surface, removing sulfides into the overlying waters. Deletion of the irrigation component produced the highest levels of dissolved sulfides

across all fluxes during production, with a value of  $4300\mu\text{M}$  at  $1\text{gC m}^{-2}\text{ d}^{-1}$  reaching an apparent maximum  $\sim 13,000\mu\text{M}$  at  $10\text{gC m}^{-2}\text{ d}^{-1}$ . During following, all three depositional fluxes displayed low sulfide values for deletion of  $D_b$  and for elimination of sulfide toxicity. In contrast, sulfide values remained high at following across all three depositional fluxes

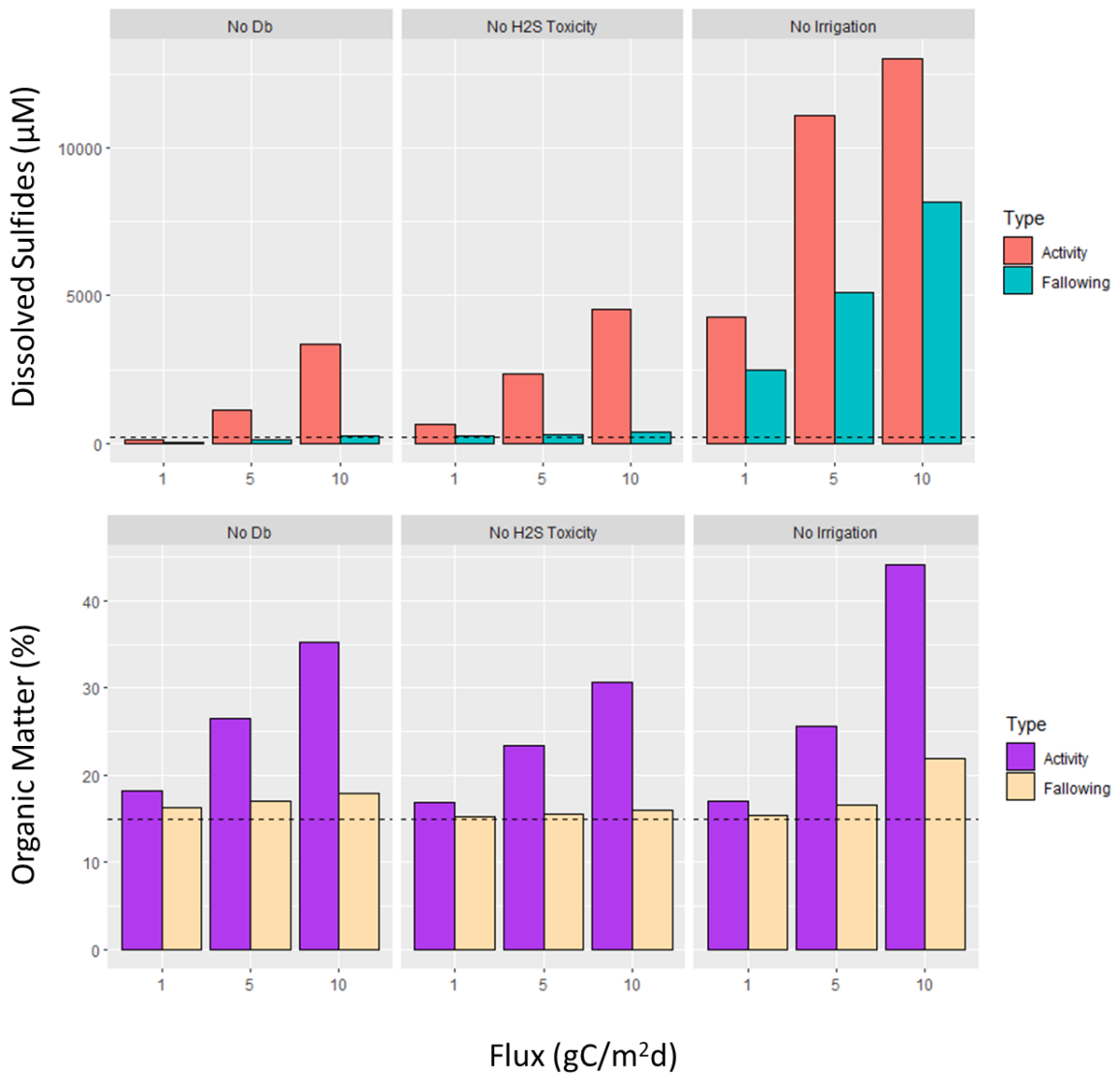


Figure 3.5: Dissolved sulfides and organic matter content for simulations run with **elimination of various transport parameters**. ‘Activity’ simulations run for 15 months and, ‘Following’ simulations run for 6 months, with initial Following profiles taken from final Activity simulation output. Horizontal dashed line = initial conditions.

(2450-8150 $\mu$ M) when bioirrigation was removed presumably due to continued sulfate reduction on buried labile organic matter.

In absence of  $D_b$ , POM concentrations did not share the same pattern of low values as sulfides, instead producing relatively high concentrations. This was expected since transport of solids was affected to a lesser extent than solutes by  $D_b$ . In the absence of  $H_2S$  toxicity, patterns of outputs during culture were similar to that of the deleted  $D_b$  case for each depositional flux. For the removal of irrigation, increases in POM content during production were similar to the other scenarios except at the highest deposition rate where lack of irrigation allowed increased burial of POM. Similarly, during fallowing, deletion of  $H_2S$  toxicity allowed a POM return to ambient levels, whereas deletion of  $D_b$  retained higher POM. Lack of irrigation reduced solid transport, leaving higher levels of POM in the upper sediment.

### *3.3.5 Validation*

While the model results for a  $5gC\ m^{-2}\ d^{-1}$  deposition flux fit observations well, notable differences between Sandy and Hartz in POM and sulfide aggregate values produced different fits for each site. Differences between the two sites were most notable when comparing sulfides. All observed sulfide values at Sandy were much higher than Hartz. Though depth, bottom type, and culturing practices at both sites were similar, response to benthic loading was highly variable. At Sandy, the observed mean sulfide during production was within  $1000\mu$ M of the simulated value; well within one standard deviation (Figure 3.6A). Simulated sulfide values were above respective observations of ambient and fallow means for both sites but fell within one standard deviation of the observed mean. Comparisons of productivity values at Hartz showed a simulated value that

fell just beyond one standard deviation from the observed mean (Figure 3.6C). However, this simulation was only representative of one depositional flux, a reduction in deposition rate would reduce the simulated sulfide value to levels similar to those observed at Hartz without reducing POM below ambient levels.

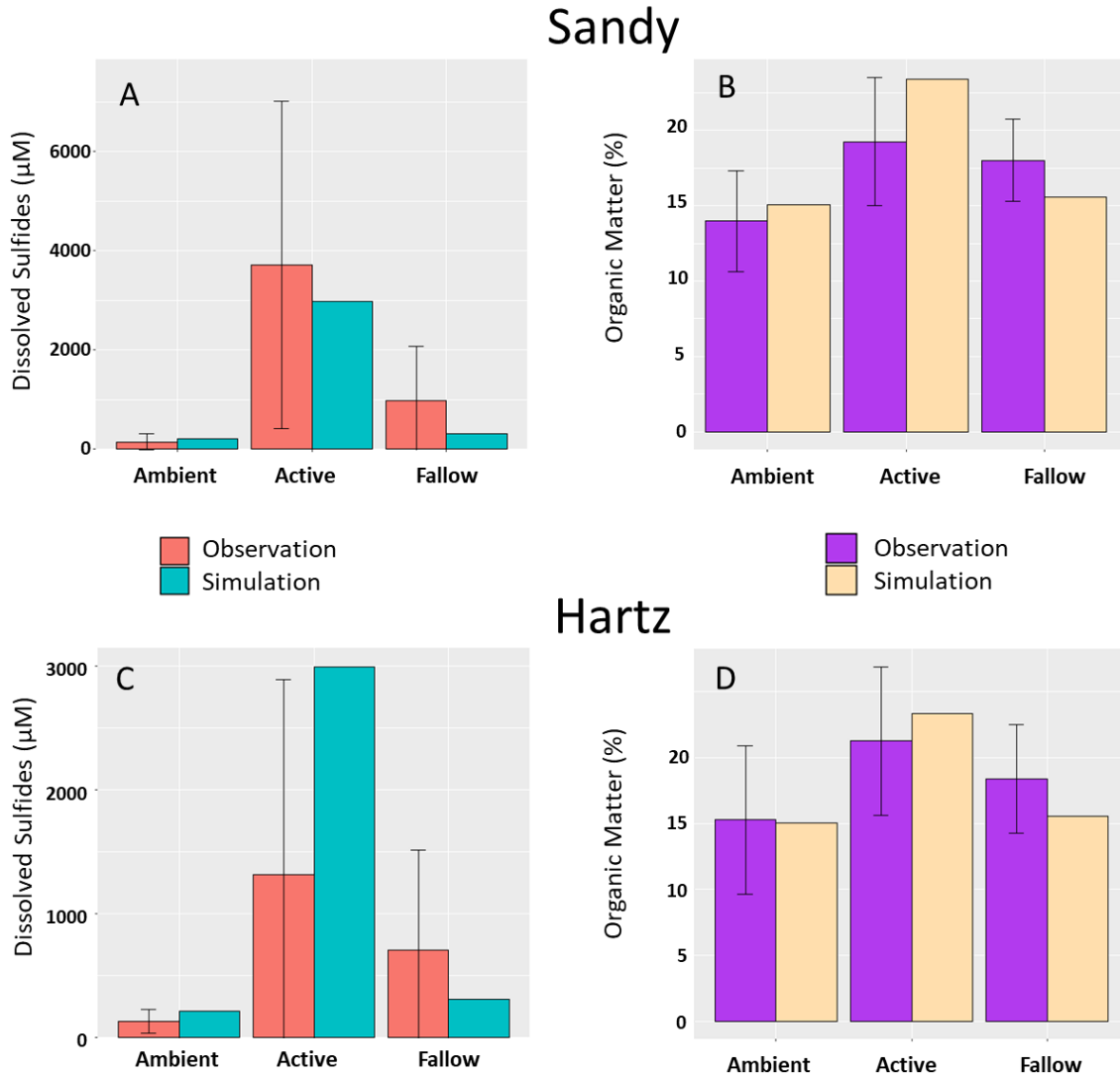


Figure 3.6: Simulation comparison to field observations from Shelburne Harbour. A & B = Sandy Point lease, C & D = Hartz Point lease. A & C = dissolved sulfides ( $\mu\text{M}$ ), B & D = organic matter (%); bars represent mean site mean; error bars represent standard deviation. Simulation parameter adjustments were as follow: Porosity = 0.75, Labile flux =  $42 \mu\text{mol}/\text{cm}^2\text{d}$  Semi-Labile Flux =  $4.5 \mu\text{mol}/\text{cm}^2\text{d}$ , and Refractory Flux =  $0.85 \mu\text{mol}/\text{cm}^2\text{d}$ ; resulting in initial conditions of OM = 15.05% and Dissolved Sulfides =  $204 \mu\text{M}$ .

EMP observations of POM content displayed high but variable values for all culture states at Hartz (Figure 3.6D) compared to Sandy (Figure 3.6B). However, increases in POM percentage from ambient to production states were similar between Hartz and Sandy. Simulated POM values were within one standard deviation of the observed mean for all culture states at both sites.

### 3.3.6 Sensitivity

Sensitivity testing results produced minimal changes to response variables from parameter variation, indicating stability within the DIAGENIX model. At a  $5\text{gC m}^{-2} \text{d}^{-1}$  farm flux,  $\pm 10\%$  parameter variations in solute boundary conditions, mineralisation rates, reaction coefficients, transport, and  $C_{\text{org}}$  content of POM resulted in  $< 20\%$  change for all response variables of concern. The response variables of greatest interest were the amount of mineralisation for each of the three pathways, total organic carbon (TOC), total dissolved sulfides, and total sulfate. However only the mineralisation rate of the semi-labile pool ( $k_{\text{OM}_2}$ ) caused a variable response  $>10\%$  (17%), when rate was reduced by 10%, and only for TOC. Though the semi-labile pool only made up 20% of total deposition flux, the response to a -10% variation in the respective rate parameter was much greater than all others assessed.

## 3.4 Discussion

The ability of DIAGENIX to forecast responses in dissolved sulfide and POM accumulation to organic enrichment is a novel approach to aquaculture site management. There is a long history of benthic geochemical models inclusive of the sulfur cycle (Paraska et al., 2014), and it is surprising that this approach has not been employed before,



considering the importance of sulfides to aquaculture management in Canada and elsewhere. Although simplification of reaction-transport processes in the sediment was necessary to reduce runtime, simulation results show promise in their ability to reflect real-world scenarios. Gaps in data availability for validation produced uncertainty, but the combination of measurements made in similar environments from previous studies and available historical records for coastal Nova Scotia allowed successful constraint of parameters and variables. In its current state, DIAGENIX addresses mineralisation and accumulation of  $C_{org}$  and resulting dissolved sulfides from aquaculture; these are major areas of interest for regulator decision making.

#### *3.4.1 Farm Deposition & Mineralisation*

Although particulate deposition was used as a net flux to the sediments, differences between the gross deposition rate from the farm and net accumulation of POM on the bottom exist. This difference is primarily the result of resuspension, where POM that has settled onto the sediment surface is repeatedly transported back into the water column through bottom current activity, reducing accumulation. Since resuspension rates are not universal, previous empirical relationships between gross deposition of POM and dissolved sulfides (Hargrave, 2010) cannot be used to validate DIAGENIX, since it is only the net accumulation of POM that is available for diagenetic reactions. A previous study quantified gross deposition and net accumulation rates of POM in Shelburne Harbour based on variable resuspension parameters (Bravo & Grant, 2018). While the relationships between gross deposition and net accumulation rate were different for each scenario, the same relationship between net accumulation rate of POM and dissolved sulfides was always produced due to the independence from hydrodynamic activity. Bravo & Grant (2018)

estimated a maximum net accumulation of POM for Shelburne at  $0.62\text{gC m}^{-2}\text{ d}^{-1}$  before sulfide concentrations  $>1500\mu\text{M}$  would occur, a rate lower than values simulated in the present study. Working ‘backward’ in a similar way with DIAGENIX suggested the maximum net accumulation rate was  $3.29\text{gC m}^{-2}\text{ d}^{-1}$ . This discrepancy was the result of DIAGENIX requiring higher mineralisation rates to achieve levels of sulfide and POM similar to those found in the EMP observations. The DIAGENIX result indicates that our use of  $5\text{gC m}^{-2}\text{ d}^{-1}$  model input for use in comparisons to EMP data was reasonable.

Components of the model such as mineralisation rate and composition of the organic pool ratios are difficult to make site-specific but are also not likely to be universal. Incubation studies have been used to measure reactivity of multiple POM pools in the past (Westrich & Berner, 1984; Grant & Hargrave, 1987; Grossi et al., 2003; Dai et al., 2009), but differences in refractory content of organic sources can produce different reactivities for each pool type when comparing single and multi-G models (Grant & Hargrave, 1987). Nonetheless, the primary origin of POM in this case is fish feces and fragmented food and their composition is well known. Previous studies have examined mineralisation rate of fish waste as well as benthic metabolism in fish farm sediments and have found these values to be relatively high compared to ambient decomposition of POM (Holmer & Kristensen, 1992; McGhie et al., 2000; Sutherland et al., 2001; Bravo & Grant, 2018). Mineralisation rates utilized in other biogeochemical models ranged from refractory/semi-labile values of  $5.5\times 10^{-9}\text{ d}^{-1}$  (Devallois et al., 2008) to  $3.0\times 10^{-3}\text{ d}^{-1}$  (Hochard et al., 2010), and labile values of  $2.5\times 10^{-3}\text{ d}^{-1}$  (Katsev et al., 2006) to  $0.83\text{ d}^{-1}$  (Fossing et al., 2004). POM pools were assigned mineralisation rates that fell near or within these limits while maintaining values that allowed for sufficient  $\text{C}_{\text{org}}$  burial and production of sulfides similar

to those found in EMP data. In simulations of variable mineralisation rates, the concentration of sulfide compared to POM increased with deposition flux, however no discernable positive or negative trends between mineralisation rates and rate of accumulation of sulfide or POM content were present for final outputs. When comparing mineralisation rates, the complexity of the modelled sediment causes variable time lags of response in reaction-transport processes for the same deposition flux (Soetaert et al., 1996a), often resulting in changes to what mineralisation rate produces the highest concentration of sulfide compared to POM at each time step during the simulation. Conversely, the consistent positive relationship present between concentration of sulfide compared to POM and labile content of the deposition flux suggests a greater temporal synchronicity for rates of change within these parameters than those of mineralisation rates. Though DIAGENIX and recent models have become increasingly separated from validating mineralisation rates through laboratory studies due to complexity (Paraska et al., 2014), a constrained range of mineralisation rates would be sufficient for inclusion of DIAGENIX into management strategies when combined with empirical data.

### *3.4.2 Validation*

Despite this simplified view of POM, DIAGENIX was successful at predicting organic content of the sediment. Since POM arises from a variety of sources with different reactivities, it should be difficult to parameterize. Using a 40%  $C_{org}$  proportion of total POM for all reactive pools, modelled sulfide and POM values were able to capture the range of reported EMP observations in Shelburne Harbour. Though some  $10\text{gC m}^{-2} \text{d}^{-1}$  deposition simulations produced POM content greater than the highest reported EMP observation, simulation limits of deposition flux only represent those values required in

reporting for AAR regulations, not the limits of real-world scenarios. In addition, other forms of benthic metabolism can consume POM and influence EMP observations (e.g. manganese reduction and denitrification), but they were not in the model. Beyond geochemical considerations, EMP sampling for POM occurs only at the cage edge, ignoring diminishing gradients of deposition outward from the center of cages, leaving important sections of the benthos unobserved. Future coupling of DIAGENIX to a deposition model will alleviate this mismatch, providing more accurate POM deposition rates at cage centers.

Differences in field observations of sediment variables for two ostensibly similar sites, Hartz and Sandy, highlight the factors that affect benthic conditions. While some of these differences could be attributed to hydrodynamics, the two sites were in close enough proximity to minimize this influence. It was assumed that both sites would be operating at near-maximum allowable biomass although the details of stocking density and cage size were not known. Sandy however had significantly greater sulfide accumulation than Hartz. During the EMP period 2004-2019, Hartz was cultured for 6 years compared to 9 years at Sandy. Fish farming has occurred in Shelburne Harbour since the 1980's, and site history previous to the EMP data is unknown.

Like POM, the range of simulated sulfide outputs were able to cover nearly all reported EMP values between 2004-2019 assuming depositional fluxes were  $\leq 5\text{gC m}^{-2} \text{d}^{-1}$ , with minimal exceptions. However, simulations were run for only one culture year, did not consider prior accumulation of POM or the potential diffusion of sub-surface dissolved sulfides from previous years, and due to the lack of husbandry information culture production data at both sites before and after 2004, the effect of historical particulate

sulfides could not be included. Since EMP sampling utilizes an integrated sample from the top 2cm of the sediment column, a large component of the sediment column, where reactions and transport involving sulfide and POM still occur, is ignored. These unmonitored sediments can influence sulfide accumulation rates and are difficult or impossible to determine through analyses that only consider the upper 2cm. Additionally, the sulfate pool can become rapidly depleted given high  $C_{org}$  flux to the sediment (Jørgensen & Kasten, 2006). When sulfate reaches low levels in deeper sediments, methanogenesis takes over as the dominant pathway, affecting both sulfide production rate and POM accumulation for DIAGENIX which does not include this pathway. When a depositional flux of  $10\text{gC m}^{-2}\text{ d}^{-1}$  was applied to DIAGENIX, sulfate became fully depleted throughout the entire 30cm domain in  $\sim 3$  years time.

Procedures for dissolved sulfide measurement used in the EMP and this study rely on the ion-selective electrode (ISE) method, where the potential of a silver/sulfide electrode within a slurry of sediment and porewater is correlated with sulfide ion activity (AAR, 2018). While this method has been frequently adopted due to its relative accessibility, bias can arise due to the addition of the alkaline buffer required to stabilize the samples (Hseu & Rechnitz, 1968; Brown et al., 2011; Cranford et al., 2017; Cranford et al., 2020). Alkaline conditions may cause dissolution of particulate sulfide ( $\text{FeS}$ ,  $\text{FeS}_2$ ) into  $\text{S}^{2-}$ , which then becomes detectable by the ISE (Brown et al., 2011). Iron-sulfides are some of the most important sinks for sulfides (Jørgensen & Kasten, 2006), and a long active site could have larger reserves of these minerals.

Filling the gaps in the data available for validation would likely produce more accurate and precise predictions at future sites, however current results will provide

valuable baselines to be incorporated with data collection tailored to address these shortcomings. The acquisition of empirical data on culturing, carbon content of POM, sediment profiles, and sulfide content through alternative procedures are all viable for inclusion in successive validations with the proper planning.

### *3.4.3 Biological Transport*

The importance of biologically mediated transport on sediment biogeochemistry is well known (Davis, 1974; Aller & Aller, 1998; Wenzhofer & Glud, 2002), and can heavily influence exchanges between the sediment and water column (Hammond & Fuller, 1979; Christensen et al., 1984; Archer & Devol, 1992). Models that incorporated irrigation through increased  $D_b$  values or nonlocal exchange, as in DIAGENIX, have been successfully validated when solute transport was dominated by irrigation (Soetaert et al. 1996b; Wang & Van Cappellen, 1996). Simulations where irrigation and  $D_b$  were removed produced the upper and lower bounds of relationships between concentration of sulfide compared to POM in relation to deposition flux, respectively. In removing  $D_b$  from the model, the burial of solids was significantly reduced, keeping POM near the SWI, and rapidly removing sulfides. Though removal of  $D_b$  showed the slowest increase in concentration of sulfide compared to POM in relation to deposition flux, the trend was near-linear like most other simulations. Benthic response was weakened most extensively when irrigation was removed, illustrated by the highest values of sulfide accumulation during production. Unlike  $D_b$ , removal of irrigation displayed the most rapid increase in concentration of sulfide compared to POM for lower deposition fluxes, however higher deposition fluxes actually reduced the sulfide accumulation response compared to lower deposition fluxes. This lower return on sulfide content above a certain deposition flux

displays a notable deviation from other simulations and highlights the difference in influences of solid and solute transport. The differences between removal of  $D_b$  and irrigation provide further limits to DIAGENIX and offer insight on how a system that has already succumbed to a complete loss of biological activity might react to additional POM deposition.

The inclusion of a term which limits bioturbation and bioirrigation based on sulfide toxicity provided an optimized control of the biological transport parameters. Initial incursions of dissolved sulfides into irrigation burrows can actually enhance bioirrigation velocities through a dominant species regime change to one more tolerant of sulfides with differing irrigation patterns (Wang & Chapman, 1999; Heilskov et al. 2006). However, upper bounds for sulfide tolerances are finite, and therefore the overall trend would be an inverse relationship between biological activity and sulfide concentration, as in DIAGENIX. In simulations, the rate at which sulfide toxicity would reduce biological transport was not only based on the rate of sulfide production from fresh POM deposition near the surface, but also the sulfide content below the biological domain. In absence of toxic concentrations, sulfide was rapidly removed through irrigation after diffusing upwards into the biological domain. However, once high levels of sulfide accumulation began to occur near the sediment surface, irrigation was mitigated throughout. Reduction in irrigation slowed sulfide removal from the biological domain, leading to further accumulation of sulfides and reduction in irrigation, with a rate inversely related to sulfide content below the biological layer. The window of time in which a complete collapse of irrigation within the system occurred was easily detectable, as values could increase by 5,000-8,000 $\mu$ M in a matter of days. This was contrasted by the simulations where sulfide

toxicity was absent, and a near-linear relationship between deposition flux and concentration of sulfide compared to POM was present. Though the sulfide toxicity term reduced the complexity of the biological domain, a rapid change to response in sulfide and POM accumulation would not be unexpected in a real-world scenario where transport of solutes was strongly reliant on biology.

#### *3.4.4 Recovery*

Sedimentary studies of fallowing at aquaculture sites frequently contain methods composed of a combination of biodiversity and geochemical indicators. While studies that include only biodiversity indicators are not uncommon (Ritz et al., 1989; Lin & Bailey-Brock, 2008), those that also include geochemical measurements offer a more complete picture (Brooks et al., 2003; Brooks et al., 2004; Macleod et al., 2006; Aguado-Gimenez et al., 2012; Keeley et al., 2013; Keeley et al., 2014; Keeley et al., 2015). Differences in geochemical recovery time to oxic conditions have been found to vary from four months (Brooks et al., 2003) to five (Keeley et al., 2014) to six years (Brooks et al., 2004). In the DIAGENIX model, farm deposition  $\leq 5\text{gC m}^{-2} \text{d}^{-1}$  recovered to sulfide values similar to initial state well within the 6 month fallow period, even when hypoxic values were observed during production, with the exception of the simulation where irrigation was removed. However, a transition to oxic from hypoxic categorization may not imply that the system had returned to ambient-state, since EMP observations include only the upper sediment. Lingering sulfide minerals are oxidized as sediments become more oxic during fallow, and  $C_{\text{org}}$  in the deeper sediments could impact future rates of accumulation in the upper sediments if farming is reintroduced too rapidly. For example, a delayed upward flux of buried sulfide towards the sediment surface potentially occurred at the Sandy lease in



2013 when observed sulfide values increased from the previous year when no production had occurred since 2011 (Milewski, 2013). In DIAGENIX, deeper sulfides would in turn reduce the overall recovery rate of the biological domain, keeping biological transport rates lower than what occurred at ambient state. Though sulfides increased from 2012 to 2013 at Sandy, the overall trend in sulfide concentration was downward from 2011-2013, however both biodiversity and abundance continued to decline during this time (McGregor Geoscience Ltd., 2012; McGregor Geoscience Ltd., 2013; Milewski, 2014), suggesting a slower recovery rate, as in DIAGENIX.

#### *3.4.5 Future Applications*

Ultimately, DIAGENIX has potential to be a useful tool in any high depositional flux environment. Although we used categories of 1, 5, and 10gC m<sup>-2</sup> d<sup>-1</sup> for depositional input to DIAGENIX, in practical application of the diagenetic model there will be a depositional model (ORGANIX; Cubillo et al., 2018) that more accurately predicts deposition based on fish biomass. Future usage of the model will be coupled to waste deposition and hydrodynamic models in the software framework under design called FINS (Farm Interactions in Natural Systems). However, the differences between gross deposition and net accumulation of POM will need to be addressed to increase accuracy of DIAGENIX compared to field observations. Although the focus of the present study was on the net accumulation of sulfides through sulfate reduction, the model design allows for the ability to track percent aerobic respiration for each simulation (Appendix A.1). While simulated values of sulfide and POM in surface sediments might appear similar to reference values, it is the comparison of sulfate and aerobic mineralisation rates which can best

determine response to future loading; a strong addition in attempts to determine benthic health.

FINS can be utilized by a variety of stakeholders within the aquaculture industry at large, helping drive decision making throughout the life of the lease. There is always a danger of a lease being surrendered back to the province if anoxia cannot be properly mitigated, resulting in losses of millions of dollars in revenue. Therefore, ability to assure aquaculture lease stakeholders that their management choices would not push the sediment beyond oxic conditions would be valuable. Simulation results from the present study have provided evidence to the assertion that benthic field samples alone are insufficient in forecasting biological activity in marine sediments throughout the farming season unless properly paired with ongoing modelling.

## **CHAPTER 4**

### **Conclusions**

When it comes to defining acceptable levels of waste into an environment, it can be difficult to find a balance between the natural system, regulating bodies, and corporate interests. While corporate interests are solely responsible for taking actions which directly or indirectly stimulate industry growth, regulators are responsible for maintaining a large variety of connected ecosystem services that the public deem valuable. However, both groups deal with limits in understanding of the ecosystem and resources to take effective action. Certain ecosystems can have high levels of resiliency, able to assimilate and remove large amounts of pollutants, whereas others are sensitive to mild disruptions. While generalized methods for regulating aquaculture sites at the federal or provincial scale present a suitable framework around which a monitoring program can be built, this research showed that considerations should be made on different spatiotemporal scales and in predictive modelling for individual leases.

Chapter 2 highlighted the diversity in response to organic loading between three sites within the same bay. During the high-frequency sampling in 2019, sites showed little indication of organic loading in the early months following stocking. However, patterns changed in the late summer and fall when the extent of the depositional footprint at each site began to become apparent. This suggests that the sampling frequency was excessive in the early months and may have been better suited to the later half of the culturing season. The natural variability of the three leases was inconsistent between sites due to the unique heterogeneity of each benthic system, but different responses in dissolved sulfide and POM accumulation allowed distinctions to be made. The sulfide content relative to redox

potential at all sites was greater than the empirical relationships used to define the benthic health categorizations used by the province, suggesting the potential need for method revision. The placement of the McNutts lease in the outer bay allowed for it to host a greater content of fish than Sandy and Hartz, but the site was still susceptible to large accumulations of sulfides. Further research is necessary into the potential causes for the difference in response of the two inner bay sites to similar levels of organic loading. The more sensitive site at Sandy Point should be restricted in the upper threshold for allowable biomass compared to Hartz.

Chapter 3 presented the potential of DIAGENIX as a forecasting model for aquaculture management. Results provided a comparison to the two inner bay lease sites at a mid-rate depositional flux, and changes to the relationship between POM and sulfide content resulting from important reaction and transport parameter tunings. Unfortunately, limited EMP data prevented more precise tunings of the model to better reflect culturing timelines throughout the life of each lease, requiring the validation method to utilize aggregates of ambient, productivity, and fallowed observations. However, model results reflected observations well, with the majority of EMP values falling within the range of model outputs. As was identified in Chapter 2, the benthic responses to organic loading at Sandy and Hartz produced different relationships between sulfide and POM content, resulting in a different fit at each site. Assuming similar culturing practices and net accumulation of POM at each site, these differences in fit display potential confidence of the model.

While this work produced useful analyses for the future refinement of aquaculture monitoring methods, further work is required. Though a best-fit sampling resolution was

not determined, evidence was provided to the hypothesis that the current sampling regime was insufficient. However, as previously stated, it is understood that a balance must be struck and oftentimes sampling frequency is reliant on availability of human resources. The ability of DIAGENIX to be a useful tool is evident, but certain site-specific observations must be made before it can be applied to sites in the future.

## **WORKS CITED**

- Adams, T. P., Black, K., Black, K., Carpenter, T., Hughes, A., Reinardy, H. C., Weeks, R. J. (2020). Parameterising resuspension in aquaculture waste deposition modelling. *Aquaculture Environment Interactions*, 12, 401-415.
- Aguado-Giménez, F., Piedecausa, M. A., Gutierrez, J. M., Garcia-Charton, J. A., Belmonte, A., Garcia-Garcia, B. (2012). Benthic recovery after fish farming cessation: a 'beyond-BACI' approach. *Mar. Pollut. Bull.*, 64, 729–738.
- Aller, R.C. & Aller, J.Y. (1998). The effect of biogenic irrigation intensity and solute exchange on diagenetic reaction rates in marine sediments. *J. Mar. Res.*, 56, 905–936.
- Archer, D., & Devol, A. (1992). Benthic oxygen fluxes on the Washington shelf and slope—A comparison of in situ microelectrode and chamber flux measurements. *Limnol. Oceanogr.*, 37, 614–629.
- Aquaculture Activities Regulations. (2018). Aquaculture Activities Regulations Monitoring Standard. Retrieved from the Fisheries and Oceans Canada website: <https://www.dfo-mpo.gc.ca/aquaculture/management-gestion/doc/AAR-Monitoring-Standard-2018-eng.pdf>
- Barbera, A. C., Vymazal, J., Maucieri, C. (2019). Greenhouse gases formation and emission. *Encyclopedia of Ecology*, 2, 329-333.
- Beulig, F., Røy, H., Glombitza, C., Jørgensen, B. B. (2018). Control on rate and pathway of anaerobic organic carbon degradation in the seabed. *Proc. Natl. Acad. Sci. U.S.A.*, 115, 367–372. doi: 10.1073/pnas.1715789115
- Beveridge, M. C. M. (1987). *Cage Aquaculture*. Fishing News Books Ltd., Cambridge.
- Boudreau, B. P. (1986). Mathematics of tracer mixing in sediments: I. Spatially dependent, diffusive mixing. *Amer. Jour. Sci.*, 286, 161-198.
- Boudreau, B. P., (1996). A method-of-lines code for carbon and nutrient diagenesis in aquatic sediments. *Comput. Geosci.*, 22, 479-496.
- Boudreau, B. P. (1997). *Diagenetic models and their implementation: modelling transport and reactions in aquatic sediments*. Springer-Verlag, Berlin.
- Boudreau, B. P., Huettel, M., Forster, S., Jahnke, R. A., McLachlan, A., Middelburg, J. J., Nielsen, P., Sansone, F., Taghon, G., Van Raaphorst, W., Webster, I., Weslawski, J. M., Wiberg, P., Sundby, B. (2001). Permeable marine sediments: overturning an old paradigm. *EOS*, 82, 133-136.

- Bravo, F. (2017). *Multi-scale assessment and simulation of sediment biogeochemical cycles in coastal areas: implications for ecosystem function and provision of services*. [Doctoral dissertation, Dalhousie University]
- Bravo, F. & Grant, J. (2018). Modelling sediment assimilative capacity and organic carbon degradation efficiency at marine fish farms. *Aquaculture Environment Interactions*, *10*, 309-328.
- Brown, K. A., McGreer, E. R., Taekema, B. (2011). Determination of free sulphides in sediment porewater and artefacts related to the mobility of mineral sulphides. *Aquat. Geochem.*, *17*, 821–839.
- Brooks, K. M., Stierns, A. R., Mahnken, C. V. W., Blackburn, D. B. (2003). Chemical and biological remediation of the benthos near Atlantic salmon farms. *Aquaculture*, *219*, 355–377.
- Brooks, K. M., Stierns, A. R., Backman, C. (2004). Seven year remediation study at the Carrie Bay Atlantic salmon (*Salmo salar*) farm in the Broughton Archipeligo, British Columbia, Canada. *Aquaculture*, *239*, 81–123.
- Burke, M., Grant, J., Filgueira, R., Stone, T. (2021) Oceanographic process control dissolved oxygen variability at a commercial Atlantic salmon farm: Application of a real-time sensor network. *Aquaculture*, *533*, 736143.
- Canfield, D. E. (1989). Sulfate reduction and oxic respiration in marine sediments: implications for organic carbon preservation in euxinic environments. *Deep-Sea Res.*, *36*, 121-138.
- Chamberlain, J., & Stucchi, D. (2007). Simulating the effects of parameter uncertainty on waste model predictions of marine finfish aquaculture. *Aquaculture*, *272*, 296-311.
- Chang, B. D., Page, F. H., Losier, R. J., McCurdy, E. P. (2014). Organic enrichment at salmon farms in the Bay of Fundy, Canada: DEPOMOD predictions versus observed sediment sulfide concentrations. *Aquaculture Environment Interactions*, *5*, 185–208.
- Christensen, J. P., Devol, A. H., Smethie, W. M. (1984). Biological enhancement of solute exchange between sediments and bottom water on the Washington shelf. *Cont. Shelf Res.*, *3*, 9–23.
- Cranford, P. J., Anderson, R., Archambault, P., Balch, T., Bates, S., Bugden, G., Callier, M. D., Carver, C., Comeau, L. A., Hargrave, B., Harrison, W. G., Horne, E., Kepkay, P. E., Li, W. K. W., Mallet, A., Ouellette, M., Strain, P. (2006). *Indicators and thresholds for use in assessing shellfish aquaculture impacts on fish habitat*. (DFO Can Sci Advis Sec Res Doc 2006/034) Canadian Department of Fisheries & Oceans, Ottawa.

- Cranford, P. J., Brager, L., Wong, D. (2017). A dual indicator approach for monitoring benthic impacts from organic enrichment with test application near Atlantic salmon farms. *Marine Pollution Bulletin*, 124, 258-265.
- Cranford, P., Brager, L., Elvines, D., Wong, D., Law, B. (2020). A revised classification system describing the ecological quality status of organically enriched marine sediments based on total dissolved sulfides. *Marine Pollution Bulletin*, 154, 111088. doi: <https://doi.org/10.1016/j.marpolbul.2020.111088>
- Cromeey, C. J., Thetmeyer., H., Lampadariou, N., Black, K. D., Kogeler, J., Karakassis, I. (2012). MERAMOD: predicting the deposition and benthic impact of aquaculture in the eastern Mediterranean Sea. *Aquacult Environ Interact*, 2, 157–176.
- Cromeey, C. J., Nickell, T. D., Black, K. D. (2002). DEPOMOD – modeling the deposition and biological effects of waste solids from marine cage farms. *Aquaculture*, 214, 211–239.
- Dai, J., Sun, M.-Y., Culp, R. A., Noakes, J. (2009). A laboratory study on biochemical degradation and microbial utilization of organic matter comprising a marine diatom, land grass, and salt marsh plant in estuarine ecosystems. *Aquatic Ecology*, 43(4), 825-841.
- Davis, R. B. (1974). Tubificids alter profiles of redox potential and pH in profundal lake sediments. *Limnol. Oceanogr.*, 19, 342–346.
- Devallois, V., Boyer, P., Boudenne, J., Coulomb, B. (2008). Modelling the vertical profiles of O<sub>2</sub> and pH in saturated freshwater sediments. *Ann. Limnol.*, 44, 275-288.
- DFO. (2012). *Review of DEPOMOD predictions versus observations of sulfide concentrations around five salmon aquaculture sites in southwest New Brunswick* (Rep. 2012/042). DFO Can. Sci. Advis. Sec. Sci. Advis. <https://waves-vagues.dfo-mpo.gc.ca/Library/347527.pdf>.
- Diaz, R. J., & Rosenberg, R. (2008). Spreading dead zones and consequences of marine ecosystems. *Science*, 321(5891), 926-929.
- Dhakar, S. P., & Burdige, D. J. (1996). Coupled, non-linear, steady state model for early diagenetic processes in pelagic sediments. *Am. J. Sci.*, 296, 296-330.
- Folk, R. L., Ward, W. C. (1957). A study in the significance of grain-size parameters. *Journal of Sedimentary Petrology*, 27, 3-26.



- Fossing, H., Berg, P., Thamdrup, B., Rysgaard, S., Sørensen, H. M., Nielsen, K. (2004). *A model set-up for an oxygen and nutrient flux model for Aarhus Bay (Denmark)*. (NERI Technical Report No. 483). National Environmental Research Institute, Denmark.
- Froehlich, H. E., Gentry, R. R., Rust, M. B., Grimm, D., Halpern, B. S. (2017). Public perceptions of aquaculture: evaluating spatiotemporal patterns of sentiment around the world. *PLoS ONE*, *12*(1), 1-18.
- Giles, H. (2008). Using Bayesian networks to examine consistent trends in fish farm benthic impact studies. *Aquaculture*, *274*, 181-195.
- Grant, J., & Hargrave, B. T. (1987). Benthic metabolism and the quality of sediment organic carbon. *Biological Oceanography*, *4*(3), 243-264.
- Gray, J. S., Wu, R. S., Or, Y. Y. (2002). Effects of hypoxia and organic enrichment on the coastal marine environment. *Marine Ecology Progress Series*, *238*, 249-279.
- Greenfield, B. L., Kraan, C., Pilditch, C. A., & Thrush, S. F. (2016). Mapping functional groups can provide insight into ecosystem functioning and potential resilience of intertidal sandflats. *Marine Ecology Progress Series*, *548*, 1-10.
- Grossi, V., Caradec, S., Gilbert, F. (2003). Burial and reactivity of sedimentary microalgal lipids in bioturbated Mediterranean coastal sediments. *Marine Chemistry*, *81*, 57-69.
- Hargrave, B. T. (1994). Modeling benthic impacts of organic enrichment from marine aquaculture. *Can Tech Rep Fish Aquat Sci*, *1949*, 1-125.
- Hargrave, B. T., Phillips, G. A., Doucette, L. I., White, M. J., Milligan, T. G., Wildish, D. J., Cranston, R. E. (1997). Assessing benthic impacts of organic enrichment from marine aquaculture. *Water Air Soil Pollut*, *99*, 641-650.
- Hargrave, B. T., Doucette, L. I., Cranford, P. J., Law, B. A., Milligan, T. G. (2008). Influence of mussel aquaculture on sediment organic enrichment in a nutrient-rich coastal embayment. *Marine Ecology Progress Series*, *365*, 137-149.
- Hargrave, B. T. (2010). Empirical relationships describing benthic impacts of salmon aquaculture. *Aquaculture Environment Interactions*, *1*, 33-46.
- Hart, S. L., & Ahuja, G. (1996). Does it pay to be green? An empirical examination of the relationship between pollution prevention and firm performance. *Bus. Strategy Environ.* *1996*, *5*, 30-37.

- Heilskov, A. C., Alperin, M., Holmer, M. (2006). Benthic fauce bio-irrigation effects on nutrient regeneration in fish farm sediments. *Journal of Experimental Marine Biology and Ecology*, 339, 204-225.
- Hochard, S., Pinazo, C., Grenz, C., Evans, J. L. B., Pringault, O. (2010). Impact of microphytobenthos on the sediment biogeochemical cycles: a modeling approach. *Ecol. Model.*, 221, 1687-1701.
- Holling, C. S. (1973). Resilience and stability of ecological systems. *Annual Review of Ecology and Systematics*, 4, 1-23.
- Holling, C. S. (1996). Engineering resilience versus ecological resilience. In P. Schulze, Editor, *Engineering within ecological constraints* (pp. 31-44). National Academy Press, Washington, D.C., USA.
- Holmer, M., & Kristensen, E. (1992). Impact of marine fish cage farming on metabolism and sulfate reduction of underlying sediments. *Mar. Ecol. Prog. Ser.*, 80, 191–201.
- Hseu, T. M., Rechnitz, G. A. (1968). Analytical study of a sulfide ion-selective membrane electrode in alkaline solution. *Anal. Chem.*, 40, 1054–1060.
- Jørgensen, B. B. (1977). The sulfur cycle of a coastal marine sediment (Limfjorden, Denmark). *Limnol. Oceanogr.*, 22, 814-832
- Jørgensen, S. E., & Bendoricchio, G. (2001). *Fundamentals of ecological modelling*. Elsevier
- Jørgensen, B. B., & Kasten, S. (2006). Sulfur cycling and methane oxidation. In H.D. Horst & Z. Mabel (Eds.), *Marine Geochemistry* (pp. 271-310). Berlin; New York: Springer.
- Jørgensen, B. B., Findlay, A. J., Pellerin, A. (2019). The biogeochemical sulfur cycle of marine sediments. *Frontiers in Microbiology*, 10, 849. doi: 10.3389/fmicb.2019.00849
- Karakassis, I., Hatzianmi, E., Tsapakis, M., Plaiti, W. (1999). Benthic recovery following cessation of fish farming: a series of successes and catastrophes. *Mar. Ecol. Progr. Ser.*, 184, 205–218.
- Katsev, S., Tsandev, I., L'heureux, I., Rancourt, D.G. (2006). Factors controlling long-term phosphorus efflux from lake sediments: exploratory reactive-transport modeling. *Chem. Geol.*, 234, 127-147.

- Keeley, N. B., Cromey, C. J., Goodwin, E. O., Gibbs, M. T., Macleod, C. M. (2013). Predictive depositional modelling (DEPOMOD) of the interactive effect of current flow and resuspension on ecological impacts beneath salmon farms. *Aquaculture Environment Interactions*, 3, 275-291.
- Keeley, N. B., Macleod, C. K., Hopkins, G. A., Forrest, B. M. (2014). Spatial and temporal dynamics in macrobenthos during recovery from salmon farm induced organic enrichment: when is recovery complete? *Mar. Pollut. Bull.*, 80, 250–262.
- Keely, N. B., Forrest, B. M., Macleod, C. K. (2015). Benthic recovery and re-impact responses from salmon farm enrichment: Implications for farm management. *Aquaculture*, 435, 412-423.
- Kim, K. (2017). Proactive versus reactive corporate environmental practices and environmental performance. *Sustainability*, 10(1), 97-117.
- Kluger, L. C., Filgueira, R., Wolff, M. (2017). Integrating the concept of resilience into an ecosystem approach to bivalve aquaculture management. *Ecosystems*, 20, 1364-1382.
- Lin, D. T., & Bailey-Brock, J. H. (2008). Partial recovery of infaunal communities during a fallow period at an open-ocean aquaculture. *Mar. Ecol. Prog. Ser.*, 371, 65–72.
- Macleod, C. K., Moltschaniwskyj, N. A., Crawford, C. M. (2006). Evaluation of short-term fallowing as a strategy for the management of recurring organic enrichment under salmon cages. *Mar. Pollut. Bull.*, 52, 1458–1466.
- Macleod, C. K., Moltschaniwskyj, N. A., Crawford, C. M., (2008). Ecological and functional changes associated with long-term recovery from organic enrichment. *Mar. Ecol. Progr. Ser.*, 365, 17–24.
- Masch, F. D., & Denny, K. J. (1966). Grain size distribution and its effect on the permeability of unconsolidated sands. *Water Resources Research*, 2(4), 665-677.
- McGhie, T. K., Crawford, C. M., Mitchell, I. M., O'Brien, D. (2000). The degradation of fish-cage waste in sediments during fallowing. *Aquaculture*, 187, 351–366.
- McGregor GeoScience Ltd. 2013. Aquaculture survey and macro-invertebrate analysis report: Shelburne Harbour Sandy Point Station 1212.
- McGregor GeoScience Ltd. 2012. Aquaculture survey and macro-invertebrate analysis report: Shelburne Harbour Sandy Point Station 1115.
- Meysman, F., Middleburg, J., Herman, P., Heip, C. (2003). Reactive transport in surface sediments. II. Media: an object-oriented problem-solving environment for early diagenesis. *Computers & Geosciences*, 29, 301-318.

- Meysman, F. J. R., Boudreau, B. P., Middelburg, J. J. (2005). Modeling reactive transport in sediments subject to bioturbation and compaction. *Geochemica et Cosmochimica Acta*, 69(14), 3601-3617.
- Milewski, I. (2014). *Aquaculture survey and macro-invertebrate analysis report: 2013 Sandy Point Survey, Shelburne Harbour (Nova Scotia)*. Conservation Council of New Brunswick.
- Morse, J., & P. Eldridge. (2007). A non-steady state diagenetic model for changes in sediment biogeochemistry in response to seasonally hypoxic/anoxic conditions in the “dead zone” of the Louisiana shelf. *Marine Chemistry*, 106, 239-255.
- Nova Scotia Department of Fisheries and Aquaculture (NSDFA). (2019a). Standard operating procedures for the environmental monitoring of marine aquaculture in Nova Scotia. Nova Scotia Aquaculture Marine Environmental Program.
- NSDFA. (2019b). Environmental Monitoring Program Framework for Marine Aquaculture in Nova Scotia. Nova Scotia Aquaculture Environmental Monitoring Program.
- Omori, K., Hirano, T., Takeoka, H. (1994). The limitations to organic loading on a bottom of a coastal ecosystem. *Marine Pollution Bulletin*, 28, 73–80.
- Paraska, D. W., Hipsey, M. R., Salmon, S. U. (2014). Sediment diagenesis models: review of approaches, challenges, and opportunities. *Environmental Modelling and Software*, 61, 297-325.
- Pearson, T. H., & Rosenberg, R. (1978). Macrobenthic succession in relation to organic enrichment and pollution of the marine environment. *Oceanogr. Mar. Biol. Ann. Rev.*, 16, 229–311.
- Pereira, P. M. F., Black, K., McLusky, D. S., Nickell, T. D. (2004). Recovery of sediments after cessation of marine fish farm production. *Aquaculture*, 235(1–4), 315-330.
- Pinsky, M. L., Jensen, O. P., Ricard, D., Palumbi, S. R. (2011). Unexpected patterns of fisheries collapse in the world’s oceans. *PNAS*, 108(20), 8317-8322
- Ritz, D. A., Lewis, M. E., Shen, M., (1989). Response to organic enrichment of infaunal macrobenthic communities under salmonid seacages. *Mar. Biol.*, 103, 211–214.
- Soetaert, K., Herman, P. M. J., Middelburg, J. J. (1996a). Dynamic response of deep-sea sediments to seasonal variations: A model. *Limnol. Oceanogr.*, 41(8), 1651-1668.
- Soetaert, K., Herman, P. M. J., Middelburg, J. J. (1996b). A model of early diagenetic processes from the shelf to abyssal depths. *Geochemica et Cosmochimica Acta*, 60(6), 1019-1040.

- Soetaert, K., & Herman P. M. (2009). *A Practical Guide to Ecological Modelling. Using R as a Simulation Platform*. Springer. ISBN 978-1-4020-8623-6.
- Soetaert, K. (2009). *rootSolve: Nonlinear root finding, equilibrium and steady-state analysis of ordinary differential equations*. R package 1.6.
- Soto, D., Aguilar-Manjarrez, J., Brugère, C., Angel, D., Bailey, C., Black, K., Edwards, P., Costa-Pierce, B., Chopin, T., Deudero, S., Freeman, S., Hambrey, J., Hishamunda, N., Knowler, D., Silvert, W., Marba, N., Mathe, S., Norambuena, R., Simard, F., Tett, P., Troell, M., Wainberg, A. (2008). Applying an ecosystem-based approach to aquaculture: principles, scales and some management measures. In D. Soto, J. Aguilar-Manjarrez, and N. Hishamunda (Eds). *Building an ecosystem approach to aquaculture* (pp. 15–35). FAO/Universitat de les Illes Balears Expert Workshop. 7–11 May 2007. *FAO Fisheries and Aquaculture Proceedings, Palma de Mallorca, Spain, 14*. Rome, FAO.
- Standish, R. J., Hobbs, R. J., Mayfield, M. M., Bestelmeyer, B. T., Suding, K. N., Battaglia, L. L., Eviner, V., Hawkes, C. V., Temperton, V. M., Cramer, V. A., Harris, J. A., Funk, J. L., Thomas. P. A. (2014). Resilience in ecology: Abstraction, distraction, or where the action is? *Biological Conservation*, *177*, 43–51.
- Strain, P. M., & Hargrave, B. T. (2005) Salmon aquaculture, nutrient fluxes, and ecosystem processes in southwestern New Brunswick. In B.T. Hargrave (Ed.), *Hbd Env Chem*, *5* (M), (pp. 29-57). Springer.
- Stucchi, D., Sutherland, T-A., Levings, C., Higgs, D. (2005). *Near-field depositional model for salmon aquaculture waste*. In: *Environmental effects of marine finfish aquaculture*. Springer.
- Sutherland, T. F., Martin, A. J., Levings, C. D. (2001). Characterization of suspended particulate matter surrounding a salmonid net-pen in the Broughton Archipelago, British Columbia. *ICES J. Mar. Sci.*, *58*, 404–410.
- Thamdrup, B., Fossing, H., & Jørgensen, B. B. (1994). Manganese, iron, and sulfur cycling in a coastal marine sediment, Aarhus Bay, Denmark. *Geochim. Cosmochim. Acta*, *58*, 5115–5129. doi: 10.1016/0016-7037(94)90298-4
- Wang, Y., & Van Cappellen, P. (1996). A multicomponent reactive transport model of early diagenesis: Application to redox cycling in coastal marine sediments. *Geochimica et Cosmochimica Acta*, *60*(16), 2993-3014.
- Wang, F. & Chapman, P. M. (1999). Biological implications of sulfide in sediment – A review focusing on sediment toxicity. *Envr. Tox. And Chem.*, *18*(11), 2526-2532.
- Webster, J. T., & Taylor, J. H. (1992). Rotational dispersion in porous media due to fluctuating flow. *Water Resources Research*, *28*, 109-119.

- Weise, A. M., Cromey, C. J., Callier, M. D., Archambault, P., Chamberlain, J., McKindsey, C. W. (2009). Shellfish-DEPOMOD: modelling the biodeposition from suspended shellfish aquaculture and assessing benthic effects. *Aquaculture*, 288, 239–253.
- Wenzhofer, F., & Glud, R. N. (2002). Benthic carbon mineralization in the Atlantic: a synthesis based on in situ data from the last decade. *Deep-Sea Res. Part I-Oceanogr. Res. Pap.*, 49, 1255–1279.
- Westrich, J. T., & Berner, R.A. (1984). The role of sedimentary organic matter in bacterial sulfate reduction: The G model tested. *Limnol. Oceanogr.*, 29, 236–249.
- Whitfield, M. (1969). Eh as an operational parameter in estuarine studies. *Aquaculture*, 14(4), 547-558.
- Wildish, D. J., Akagi, H. M., Hamilton, N. & Hargrave, B. T. (1999). A recommended method for monitoring sediments to detect organic enrichment from mariculture in the Bay of Fundy. *Can Tech Rep Fish Aquat Sci*, 2286, 1–34.
- Wildish, D. J., Hargrave, B. T., Pohle, G. (2001). Cost effective monitoring of organic enrichment resulting from salmon mariculture. *ICES J Mar Sci*, 58, 469–476.
- Wildish, D. J., Hughes-Clarke, J. E., Pohle, G. W., Hargrave, B. T., Mayer, L. M. (2004). Acoustic detection of organic enrichment in sediments at a salmon farm is confirmed by independent groundtruthing methods. *Marine Ecology Progress Series*, 267, 99-105.

## **APPENDIX**

### *A.1 Clustering Validation Methods*

The silhouette for hard clustering is calculated through

$$s_i(k) = \frac{b_i - a_i}{\max(b_i, a_i)} \quad (\text{Eq. A.1})$$

where  $a_i$  is the mean dissimilarity between object  $i$  and all other objects within the same cluster, and  $b_i$  is the lowest mean dissimilarity of  $i$  to all other clusters for which  $i$  is not a member. The neighboring cluster of object  $i$  is that of the lowest mean dissimilarity. The closer the  $s_i(k)$  value is to one, the better the object  $i$  fits to the cluster. The fuzzy silhouette is calculated through

$$FS(k) = \frac{\sum_{i=1}^n (u_{ig} - u_{ig'})^\alpha s_i(k)}{\sum_{i=1}^n (u_{ig} - u_{ig'})^\alpha} \quad (\text{Eq. A.2})$$

where, in the U matrix,  $u_{ig}$  is the largest, and  $u_{ig'}$  the second largest, component of the  $i$ -th row, and  $\alpha$  is a weighting coefficient. The partition entropy is calculated using membership degree to the U matrix

$$PE(k) = - \sum_{i=1}^n \sum_{g=1}^k \frac{u_{ig} \log_a(u_{ig})}{n} \quad (\text{Eq. A.3})$$

where  $a$  is the base of the logarithm, and the optimal number of clusters is identified by the minimized index value. The partition coefficient is again calculated using membership degree to the U matrix

$$PC(k) = \sum_{i=1}^n \sum_{g=1}^k \frac{(u_{ig})^2}{n} \quad (\text{Eq. A.4})$$

where the optimal number of clusters is identified by the maximized index value.



A.2 O<sub>2</sub> vs. SO<sub>4</sub> Pathway Quantification

Table A1: Percent of total C<sub>org</sub> mineralisation for each simulation scenario by O<sub>2</sub> and SO<sub>4</sub> pathways

Simulation ID	Flux (gCm-2d-1)	% Mineralisation	
		O <sub>2</sub>	SO <sub>4</sub>
<b>Pool Ratio 9:9:2</b>	1	42.2	57.8
	5	23.6	76.4
	10	18.9	81.1
<b>Pool Ratio 14:4:2</b>	1	43.3	56.7
	5	24.6	75.4
	10	18.2	81.8
<b>Pool Ratio 4:14:2</b>	1	40.6	59.4
	5	21.9	78.1
	10	19.0	81.0
<b>Labile Decay Rate (1/d)</b>	1	54.1	45.9
	5	35.0	65.0
	10	25.2	74.8
<b>Labile Decay Rate (0.1/d)</b>	1	43.3	56.7
	5	24.6	75.4
	10	18.2	81.8
<b>Labile Decay Rate (0.04/d)</b>	1	40.3	59.7
	5	21.6	78.4
	10	18.0	82.0
<b>No Db</b>	1	75.8	24.2
	5	43.0	57.0
	10	27.0	73.0
<b>No H<sub>2</sub>S Toxicity</b>	1	43.3	56.7
	5	25.3	74.7
	10	18.0	82.0
<b>No irrigation</b>	1	32.2	67.8
	5	22.3	77.7
	10	19.2	80.8